CONF-820440--1

Excitation of Giant Resonances Via Direct Reactions

Fred E. Bertrand

Physics Division
Oak Ridge National Laboratory*
Oak Ridge, Tennessee 37830

CONF-820440--1

DE82 013473

Nuclear Physics Workshop organized by
Argentina National Atomic Energy Commission, Mar del Plata, Argentina,
April 12-17, 1982

I. Introduction

Giant resonances are manifestations of elementary modes of nuclear excitation. Since giant resonances are general properties of all nuclei, they lend themselves to description as general properties of nuclear matter. The term giant resonance has over the years come to be used nearly synonymously with the giant dipole resonance (GDR) discovered in the 1940's. However, as we know from theoretical considerations and now experimental observation, such a correspondence is largely a product of history.

In 1970 the first non-dipole giant resonance, the giant quadrupole resonance (GQR), was experimentally observed.[1] It is significant to note that the observation of this new giant resonance was not made by photonuclear reactions, the conventional means of exciting the GDR, but by direct reactions -- specifically, inelastic scattering of medium energy protons and electrons. Thus, new resonances and new techniques were simultaneously thrust upon the well established field of photonuclear physics. In the ten years since the discovery of the GQR the study of

*Operated by Union Carbide Corporation under contract W-7405-eng-26 with the U.S. Department of Energy.

so-called giant multipole resonances has grown into a bonafide subfield of nuclear physics, one that is pursued in most medium-energy nuclear physics facilities throughout the world.

In this talk I will review the current situation as regards observation of the new resonances. Since the bulk of the results have come from hadron measurements, I will concentrate on results from hadronic direct reactions. This selection is prompted by constraints of time and should not be interpreted as a negative opinion of results from electron scattering or particle capture, areas of study which have provided significant and important contributions to the new resonance field. More detailed information on this topic may be found in references 1-3.

Although this talk concentrates on non-dipole resonances, it is helpful to remind ourselves of the properties of what was for so many years the only giant resonance established experimentally. Figure 1 shows the spectrum of ^{208}Pb as seen in the (γ,n) reaction.[4] The only structure observed in the spectrum is the peak from the GDR centered at about 13.5 MeV of excitation energy. The fact that photoabsorption proceeds overwhelmingly by dipole absorption leads to such beautiful GDR spectra which are uncomplicated by competing reactions. (Excitation of the GDR is 10-100 times stronger than E2 excitation via photoabsorption. This selectivity makes photoabsorption measurements of higher multipole resonances very difficult.) As shall be seen later such clean spectra are unfortunately not the case for excitation of giant resonances via direct reactions.

Consideration of the GDR systematics established over many years can provide a guide for the search for resonances related to other modes of

nuclear excitation. Shown on fig. 2 are values[4] of the excitation energy (E_x) plotted as $E_x A^{1/3}$ MeV, the width and sum rule depletion for the GDR for many nuclei spanning the periodic table. For nuclei with mass above ~ 130, the GDR is located at the systematic energy of ~ 78 $A^{-1/3}$ MeV and most of the GDR sum rule is accounted for. For lighter nuclei the resonance energy falls steadily from the systematic value and less than 100% of the sum rule is accounted for (at least up to ~ 30 MeV of excitation). The width of the GDR is narrowest near shell closures (A=90, 144, 208) and widest for deformed nuclei (e.g., rare earth nuclei).

These systematics yield a few characteristics of giant resonances that may be useful for experimental searches for new resonances.

1) Giant resonances are general properties of nuclei.

2) The excitation energy of a giant resonance varies smoothly with nuclear mass (at least over most of the nuclear mass range).

3) Giant resonances exhaust an appreciable fraction of an appropriate sum rule.

4) Giant resonance strength is generally localized in excitation energy (more an experimental than theoretical necessity).

II. Background

Giant resonances are often considered to be highly collective modes of nuclear excitation in which an appreciable fraction of the nucleons of a nucleus move together. Indeed the motion is so collective that it is appropriate to think of these modes of excitation in hydrodynamic terms like the oscillation of a liquid drop.

Figure 3 shows a representation of several of these modes of oscillation, where L represents the angular momentum quantum number of

the mode. The monopole (L=0) mode is a spherically symmetric oscillation or compression of the nucleus; the dipole (L=1) is pictured as a motion in which the neutrons and protons oscillate in bulk against each other while the quadrupole mode is an oscillation of the spherical nucleus to oblate shape then to prolate shape. Oscillations with $L > 3$ are, of course, possible but are not shown. The nuclear fluid has neutron, proton, "spin-up" and "spin-down" components and hence, for each multipolarity (L) there are four possible combinations of these components. Modes in which neutrons and protons oscillate in phase are characterized as isoscalar modes (denoted as T=0 here) while those modes in which the neutrons and protons oscillate out of phase are called isovector (T=1). Similarly, spin-up and spin-down nucleons oscillating in phase yield S=0 modes while the so-called spin-flip modes (S=1) are produced by spin-up and spin-down nucleons oscillating out of phase. The S=0 oscillations are the electric modes while the S=1 oscillations are the magnetic modes. The well known GDR is an example of an L=1, T=1, S=0 mode of excitation, while the first 2^+ level of nuclei are examples of L=2, T=0, S=0 modes.

The collectivity of these modes (i.e., of the nuclear states that are the observable manifestation of the various modes) can be deduced by studying the transition rates for their electromagnetic excitation (or de-excitation) or by measuring the cross sections for their excitation via direct reactions such as inelastic scattering. Useful "benchmarks" for comparison are the single particle transition rates and sum rules. While the former provide an estimate for a single nucleon promoted from

one shell-model level to another, the latter tell us how much total transition strength we can expect for a mode having particular (L,T,S) values. Throughout this talk giant resonance strength will be described in terms of the energy weighted sum rule (EWSR) which is a particularly useful sum rule because it is nearly model independent. Generally, the criterion for a transition to be considered collective is that its transition rate be many ($\gtrsim$ 10) times the single particle value, in which case the transition would exhaust an appreciable fraction of the EWSR for the mode in question. As we shall see giant resonances exhaust 20%-90% of their sum rules.

For direct reactions the transition rate and the angular momentum transfer are generally deduced by comparison of measured angular distributions with those calculated by use of the Distorted Wave Born Approximation (DWBA). The analysis procedure for giant resonance states is the same as has been established for direct excitation of low-lying states. In the case of electron scattering the transition rate, B(EL), for the state in question can be directly obtained. In inelastic hadron scattering however, the situation is not nearly so direct. Comparison of the calculated cross sections with those measured, yields a quantity called the deformation parameter, β_L, as:

$$\beta_L^2 = \frac{d\sigma(L)}{d\Omega} \text{ measured } / \frac{d\sigma(L)}{d\Omega} \text{ calculated} \qquad (1)$$

If β_L is assumed to be proportional to the mass multipole moment for a uniform distribution then

$$\beta_L^2 = B(EL)\left(\frac{4\pi}{3ZR^L}\right)^2 . \qquad (2)$$

Whether or not the transition rate as directly determined in inelastic electron scattering or deduced in hadron scattering through use of equations (1) and (2) yield the same result has been an often debated topic. However, it is clear that hadron inelastic scattering is more model dependent than electron scattering. The application of the DWBA theory to giant resonance excitation by hadron inelastic scattering has been detailed by Satchler[5] and the experimental results have usually been analyzed following Satchler's formalisms. The EWSR is related to the transition rate as:

$$S_L = B(EL)(E_f - E_i) = \frac{L(2L+1)^2}{4\pi} \frac{h^2}{2m} Ze^2 \langle r^{2L-2} \rangle , \qquad (3)$$

where E_f and E_i denote the energies of the final and initial states in the transition and $\langle r^L \rangle$ is the RMS charge radius of the ground state. For T=S=0 transitions and $\langle r^L \rangle = [3/(L+3)]R^L$ for a uniform mass distribution, the EWSR for a transition of multipole L can be written as:

$$S_L = \frac{3Ah^2}{8\pi m} LR^{2L-2}$$

where m is the nucleon mass and A is the nuclear mass number.

Using equation (2) relating β_L^2 and B(EL) the following expression for β_L^2 in terms of 100% EWSR depletion is obtained (for T=S=0):

$$\beta_L^2 = \frac{2\pi h^2}{3m} \frac{L(2L+1)}{AR^2} \frac{1}{E} \sim \frac{60L(2L+1)}{A^{5/3}E} , \qquad (4)$$

if $R = 1.2\ A^{1/3}$ fm and E = excitation energy in MeV. Equation (4)

provides the limit of the EWSR for a transition of multipole L and energy E. Throughout this talk the measured giant resonance cross section will be presented as a fraction of the limit from equation (4). Sum rules for isoscalar monopole transition and isovector transitions are different and have been treated by Satchler.[5]

Figure 4 provides a representation of transitions that might comprise various electric modes. The figure schematically represents single-particle transitions between shell-model states of a hypothetical nucleus. Collective transitions result from coherent superpositions of many such single-particle transitions. Major shells are denoted as N, N+1, etc. and are separated by $\sim 1\hbar\omega$ or $\sim 41\ A^{-1/3}$ MeV. Giant resonances may be considered to result from transitions of nucleons from one major shell to another, under the influence of an interaction that orders these transitions into a coherent motion. The interaction for inelastic scattering can excite a nucleon by at most $L\hbar\omega$, or, to state it differently, the nucleon can be promoted by at most L major shells. The number of shells is either odd or even according to the parity.

Thus, the isovector giant dipole resonance (GDR) is built up of E1 transitions spanning $1\hbar\omega$. The GDR might then be expected to be located at an excitation energy of $\sim 41\ A^{-1/3}$ MeV; however, it is located at $\sim 77\ A^{-1/3}$ MeV. This difference arises from the fact that the spin and isospin dependence of the nucleon-nucleon interaction ensures that the S=T=0 collective states move down in energy, and that S=1 or T=1 states move up from the expected energy.

For E2 excitations two different classes of transitions are allowed. The first of these, with lowest energy, is comprised of transitions

within a major shell, the so-called $0\hbar\omega$ transitions. A second set is comprised of transitions between shells N and N+2, the $2\hbar\omega$ transitions. These transitions would be pushed up or down in energy from $2\hbar\omega$ for isovector or isoscalar modes respectively. While the $0\hbar\omega$, E2, excitations are identified with the familiar low-lying 2^+ levels, the $2\hbar\omega$ class carry most of the EWSR and are associated with the GQR. By similar arguments E3 excitations of $1\hbar\omega$ and $3\hbar\omega$ and E4 excitations of $0\hbar\omega$, $2\hbar\omega$ and $4\hbar\omega$ are expected.

For each class of transitions (E1, E2, etc.) the sum rule should be exhausted by the sum of the strength in all the transitions. For example, for E2 transitions the sum rule should be exhausted by the sum of the strength in the $0\hbar\omega$ and $2\hbar\omega$ transitions.

For the GDR we know 100% of the sum rule is accounted for (fig. 2). What about other multipoles? Figure 5 shows the percent of the EWSR depleted in the first 2^+ level of even-even nuclei. Except for the lightest nuclei, only $\sim$ 10-15% of the EWSR is accounted for in the first 2^+ level. Table 1 shows a few cases (from inelastic scattering) where the entire bound state excitation region ($\lesssim$ neutron separation energy) was studied. Only for ^{24}Mg is any appreciable fraction of the L=2 EWSR strength found in the bound-state region. Thus, there is good reason to expect considerable quadrupole strength to be in the $\Delta N=2$ excitations. Indeed, less than one half of the possible sum-rule strength for any multipole is located in the bound states for the nuclei studied. In fact, there were predictions[6] that the $\Delta N=2$ quadrupole strength would be appreciable and localized at an excitation energy of $\sim 60 \times A^{-1/3}$ MeV.

TABLE 1. Percentage of isoscalar EWSR multipole strength depleted in bound states of ^{24}Mg, ^{40}Ca, and ^{208}Pb.

	Multipole								
Nucleus	0	1	2	3	4	5	6	7	8
^{24}Mg			40	10	3				
^{40}Ca	0	0	14	38	7	11	1	0.2	0
^{208}Pb	0	0	20	47	14	3	3	2	1

From these brief background comments one derives a complicated picture of giant multipole resonances. For each multipolarity there may be four independent modes and for each of these modes there may be more than one class of transitions, e.g. -- for L=4, S=0, T=0 we could find a $2\hbar\omega$ and $4\hbar\omega$ giant resonance. How then do we sort out this complicated picture? The answer lies in the selectivity of the nuclear reactions we use to search for the resonances. We have already seen an outstanding example of such selectivity in the photonuclear excitation of the GDR.

Since we have said that photonuclear reactions are not especially well suited to study giant resonances other than dipole we must, of course, ask what is an appropriate technique? The answer has been through direct reactions, especially inelastic scattering, of medium energy projectiles. It has long been known that the inelastic scattering reaction provides strong excitation of low-lying collective T=S=0 states. Thus, it seems reasonable to assume that high-lying collective states of

similar modes should also be excited. Inelastic electron scattering had been used for some time to study the GDR. However, while the electron scattering mechanism (electromagnetic) is well understood the selectivity of the reaction is rather low. The use of hadrons as projectiles provides much more variety for the reactions and thus, more selectivity. This can be seen by considering the effective interaction between a nucleon in the projectile and one in the target nucleus. The interaction is both spin and isospin dependent. For example, the central part of the interaction may be written as in Table 2.

TABLE 2

$V_{TS}(i_{ij}) = V_{00}(r_{ij}) + V_{10}(r_{ij})\tau_i\cdot\tau_j + V_{01}(r_{ij})\sigma_i\cdot\sigma_j + V_{11}(r_{ij})\sigma_i\cdot\sigma_j\ \tau_i\cdot\tau_j$			
T=0 S=0	T=1 S=0	T=0 S=1	T=1 S=1
GQR 1st $2^+,3^-$	GDR	spin-flip $2^-,3^+$	M1 Gamow-Teller
	IAS		
(p,p')	(p,p')	(p,p')	(p,p')
(α,α')			
(d,d')			
	(p,n),(^{3}He,t)		(p,n),(^{3}He,t) (^{6}Li,^{6}He)

The four modes for each multipolarity arise from a different term in the effective interaction. For example, the low-lying 2^+ and 3^- nuclear

~ 7-MeV. The peaks from elastic scattering and inelastic scattering to low-lying levels are shown on a much reduced scale. It is immediately obvious that the experimental spectra we deal with in inelastic scattering measurements of multipole resonances are more complicated or, to state it differently, less clean than the photonuclear spectra used to deduce the parameters of the GDR. While the (α,α') reaction provides selectivity of T=S=0 modes, all multipolarities may be, and indeed, generally are excited. We show on the 13 degree spectrum a decomposition of the spectrum into quadrupole (GQR), and monopole resonances (GMR) and a peak from the so called low-energy octupole resonance (LEOR). These resonances are discussed in some detail below. A possible additional resonance is shown centered at ~ 24 MeV of excitation. This resonance is now known to arise from excitation of the giant octupole resonance (GOR) recently proposed from inelastic alpha, proton and helium-3 scattering.

Figures 6 and 7 serves to illustrate what is perhaps the most serious problem in inelastic scattering studies of giant resonances -- the giant resonance cross section is only a part (often a small part) of the total continuum cross section. Some assumption must be made about both the magnitude and shape of the continuum which lies under the resonance peak. It is assumed that the giant resonance cross section does not mix with the underlying continuum and the resonance peak is "stripped off" of the continuum by extrapolating the continuum magnitude and shape from higher excitation energies. I feel that cross sections for the giant resonances cannot be obtained from inelastic scattering with less than a 15-20% absolute uncertainty. We have not yet found a way to eliminate the continuum and leave just the resonance peaks.

The remainder of this discussion will be devoted to a summary of experimental results on the new giant resonances, especially the electric multipole resonances.

III. Isoscalar Giant Quadrupole Resonance

In the notation of this presentation the isoscalar giant quadrupole resonance has quantum numbers (L,T,S) = (2, 0, 0). The T=0 GQR was the first of the new giant resonances to be discovered[1] and it remains the most well studied and carefully documented. In general there is excellent agreement between various types of hadronic measurements of the GQR and in most cases agreement with electron and particle capture reactions.

Figure 8 shows inelastic spectra[8] from five targets spanning a wide nuclear mass range, bombarded by 152-MeV alpha particles. In each spectrum a broad peak is observed at an excitation energy that varies smoothly with target mass. Prior to approximately three years ago the entire peak in each nucleus was attributed to excitation of the GQR. (For the (α,α') reaction the GDR is not excited to an observable extent.) However, as will be discussed below, we now know that (at least for nuclei heavier than about A=50) the peak contains both monopole and quadrupole resonances. The identification of the resonance, i.e., the portion marked E2, as ar L=2 excitation is provided by comparison of the measured angular distributions with those calculated using the Distorted Wave Born Approximation (DWBA). The strength of the resonance in terms of percentage depletion of the EWSR is determined by the normalization of the calculated cross sections to those measured. Figure 9 shows such a comparison[8] for the five giant resonance spectra shown on fig. 8. The data

are described very well by the DWBA calculation assuming the state to be quadrupole (L=2). For all five nuclei most of the T=0, L=2, EWSR is depleted in the resonance peak.

For nuclei having $A \leq 40$ the character of the GQR changes dramatically as is seen in fig. 10. These data[9] were taken with a magnetic spectrograph which provided energy resolution considerably less than 100 keV (FWHM). For ^{40}Ca one observes a broad peak located at $\sim 63\ A^{-1/3}$ MeV (position of arrow) similar to those in heavier nuclei. However, no such broad structure is found at $63\ A^{-1/3}$ MeV in the lighter nuclei. Rather, the excitation energy region between 12 and 20 MeV contains peaks arising from excitation of a large number of individual states. Most of these peaks are attributable to L=2 excitations.[10,11] The sum of the L=2, T=0, EWSR depleted in the individual quadrupole states is found to provide a significant fraction of the total EWSR.

Systematics for the energy, width and strength (sum rule) of the T=0 GQR are presented in fig. 11. The data were mostly taken from ref. 1 and ref. 2. Where more than one measurement has been made on a given nucleus the results were averaged. In general the excitation energy for the GQR for $A \gtrsim 100$ falls at the systematic energy of $\sim 65\ A^{-1/3}$ MeV. For nuclei lighter than mass 100 there is a clear tendency for the GQR peak to fall below the systematic energy. For nuclei lighter than A=40 the energy of the strength centroid of the individual fragments has been plotted. The dashed line at $64.7\ A^{-1/3}$ MeV is taken from a recent calculation.[12]

The width of the GQR increases smoothly with decreasing nuclear mass. However, there are apparent shell effects in the data. The narrowest

resonance widths occur for A=40, 90, 142 and 208. The resonance is widest in the region of the rare earth deformed nuclei. This behavior is similar to that observed for the GDR (fig. 2) although the increase in the GQR width in deformed nuclei is not nearly as great as for the GDR. The $A^{-2/3}$ dependence of the width predicted in ref. 12 provides a good description of the data. The value of the multiplicative constant (90) has been increased from that suggested (58) in ref. 12 in order to fit the data.

The percentage of the T=0, E2 EWSR strength depleted in the GQR is shown at the bottom of fig. 11. It is to be noted that these values do not include contributions to the EWSR from low-lying ($0\hbar\omega$) quadrupole excitations. A trend to larger sum-rule depletion with increasing nuclear mass is clearly evident. For nuclei having $A \gtrsim 100$ essentially 100% of the EWSR is found to be depleted in the GQR peak ($2\hbar\omega$ transitions), while for lighter nuclei 30-50% of the EWSR is typically found in the high-lying quadrupole states. However, considerably more EWSR strength is located in the low-lying 2^+ states of light nuclei than of heavy nuclei, so that the sum of the GQR ($2\hbar\omega$) and low-lying quadrupole ($0\hbar\omega$) strengths exhaust $\sim$ 100% of the T=0, E2 EWSR in light as well as heavy nuclei.

IV. Isovector Giant Quadrupole Resonance

As pointed out earlier, excitation of T=1 (isovector) states via hadron inelastic scattering is much weaker than excitation of T=0 states. Charge exchange reactions excite T=1, S=0 states and there is evidence[13] from (n,p) measurements that the GDR is excited. However,

charge exchange reactions have yet to clearly show excitation of the isovector giant quadrupole (L=2, T=1, S=0). On the other hand, the electromagnetic (e,e') interaction provides equal strength both T=1 and T=0 excitations (all other things being equal, e.g. -- EWSR, L, E_x). For the lighter nuclei ($A \lesssim 40$), particle capture reactions provide information on isovector strength, however most of the data on the T = 1 GQR have come from inelastic electron scattering.

The left side of fig. 12 shows inelastic electron scattering spectra[14] from ^{60}Ni. The broad peak observed at ~ 32 MeV of excitation is identified as the T=1, GQR. This identification is supported by comparison of cross sections for the peak with calculated E2 form factors as shown on the right side of fig. 12 for ^{58}Ni and ^{60}Ni.

Plotted in fig. 13 are the systematics for the T=1, GQR. The data are all from inelastic electron scattering and are taken from ref. 15. Although much less data are available than for the T=0 GQR the systematics are very similar. The excitation energy follows the systematic energy 130 $A^{-1/3}$ MeV for heavier nuclei while for lighter nuclei the energy drops off. The width of the resonance increases rather smoothly as the nuclear mass decreases. The available results show that ~ 100% of the T=1, E2 EWSR is located in the resonance peak. The trend observed in the T=0, GQR for smaller depletion of the EWSR for nuclei having $A \lesssim 100$ is not seen here, within the constraints of a much smaller available data base. The EWSR depletion shown on fig. 13 are based on use of the Goldhaber-Teller model. Use of the Myers-Swiatecki model for the (e,e') form factors results in a considerable reduction (~ 30% lower) in the EWSR depletion.

V. Isoscalar Giant Monopole Resonance

Although the most thoroughly studied of the new giant resonances is the GQR, the resonance which has generated the most interest is the monopole. We discuss here the isoscalar giant monopole resonance (GMR) (L=0,T=0,S=0). Observation of the monopole, "breathing", or compressional mode of nuclear excitation is of special significance because knowledge of its excitation energy provides direct information on the nuclear compressibility. During the past few years several candidates for the E0 resonance have appeared but most have not withstood the test of further measurements. These early measurements are discussed in ref. 1. It is important to note that some early indirect evidence for an E0 resonance[16,17] placed the monopole excitation at an energy of $\sim 80 \times A^{-1/3}$ MeV, a value in agreement with those from the recent more direct observations I will describe.

The first direct observation[18] of the resonance that was later confirmed to be the GMR was made using inelastic scattering of 120 MeV alpha particles from ^{208}Pb. Those data show the presence of two broad peaks in the giant resonance region of the spectrum. A larger peak located at 11 MeV ($65 \times A^{-1/3}$ MeV), the GQR, and a smaller peak located at 13.9 MeV or $\sim 80 \times A^{-1/3}$ MeV. This latter peak is near the energy of the GDR in ^{208}Pb (13.6 MeV), however the isovector GDR will not be excited by the (α,α') reaction with nearly enough cross section to account for this new peak. A similar peak was also found[18] in ^{206}Pb, ^{209}Bi, and ^{197}Au.

Thus it was established that a here-to-fore not directly observed resonance peak was located at ~ 14 MeV for nuclei in the lead region. The obvious question was what is the nature of the peak? It is an unfortunate circumstance that the angular distributions for L=2 and L=0 excitation via the (α,α') reaction are identical in angular regions where the giant resonances are easily measured. This fact is demonstrated on fig. 14 which shows calculated monopole and quadrupole angular distributions for the $^{208}Pb(\alpha,\alpha')$ reaction using 152 MeV alpha particles. The two curves are nearly identical for angles as small as ~ 5 degrees with the L=0 curve having somewhat larger peak to valley ratios. The 120-MeV (α,α') data of reference 18 were taken in an angle range where L=0 and L=2 angular distributions are not clearly distinguishable. Shown on fig. 14 are measured cross sections for the 13.9 and 10.9 MeV resonances obtained using 152 MeV alpha particle inelastic scattering. The measured cross sections[8] for the two resonances provide good agreement with the calculations, but not positive L=0 identification.

However, as is seen in fig. 14, at very small angles the two angular distributions are out of phase and convincing identification of the L=0 component could be made. Two groups have now provided measurements[19,20] on a number of nuclei utilizing detection systems especially designed to study very small angle (down to zero degrees) inelastic alpha and helium-3 scattering.

Spectra from inelastic scattering[21] of 129-MeV alpha-particles from ^{144}Sm and ^{154}Sm at 0, 4, and 6 degrees are shown on fig. 15. It is immediately obvious from this figure that use of small angle techniques does not eliminate the problem of excitation of the underlying nuclear

continuum. Indeed the resonance to continuum ratio may be poorer at very small angles than at larger angles. Some assumption about the shape and magnitude of the continuum underneath the resonances must be made in order to extract the resonance peaks from the spectrum. However, it is apparent, even in this figure, that the shape of the giant resonance peak changes considerably with angle.

Figure 16 shows the exciting advantages to be gained with small angle measurements.[22] The giant resonance peak, after subtraction of the continuum, is shown at several small angles for the reaction $^{116}Sn(\alpha,\alpha')$ for E_α = 129 MeV. It is apparent that the centroid of the entire peak shifts and the width of the peak is not constant as the angle of observation varies, both effects being indicative of the existence of two different multipolarities within the single broad peak. The peak is shown decomposed into two components which clearly change relative magnitude rapidly with angle. The angular distributions for the two components of the resonance peak are plotted in the lower part of the figure. The lower excitation energy peak has an L=2 angular distribution while the cross sections for the higher excitation peak follows the calculated L=0 angular distribution. Such measurements have now clearly identified the peak seen earlier at larger angles as the isoscalar GMR resonance.

The small angle experiments and measurements using the (p,p') reaction[23] have now provided a significant body of information about the GMR in many nuclei.

Systematics of the monopole resonance are shown on fig. 17. The top plot shows the trend with nuclear mass number of the energy of the GMR.

As has been the case for the resonances previously discussed, for heavier mass nuclei the resonance is located at a systematic energy, in this case $\sim 80 \times A^{-1/3}$ MeV. For lighter nuclei the now familiar trend for the reasonance to be found at lower excitation energy is observed for the GMR. The width of the monopole resonance shows a tendency to broaden as the nuclear mass decreases in agreement with the trend for other giant resonances. The sum rule depletion for the monopole resonance plotted at the bottom of fig. 17 shows that all of the T=0, E0, EWSR is accounted for in nuclei as light as ^{90}Zr. However, less than half of the sum rule strength is observed for the three lighter nuclei that have been studied.

Perhaps the most interesting aspect of the GMR to be derived from these studies is the lack of observation of the monopole resonance in nuclei having $A \lesssim 50$. There are no apparent theoretical reasons to suggest that the monopole should disappear in light nuclei. On the other hand, we know the strength for other giant resonances becomes very fragmented in light nuclei. If such is the case for the GMR and the resonance is spread over many MeV of excitation energy in light nuclei, then present measurement techniques may not be sensitive enough to locate the E0 strength.

It now seems clear that the GMR has been identified and systematically observed in a wide mass range of nuclei. The question of the low sum rule depletion for mass 50-60 nuclei and the lack of observation of any E0 strength in lighter nuclei is yet to be understood.

Observation of the giant monopole resonance is of special significance since the location of the GMR yields the value of the compressibility of nuclear matter. This comes about through the relationship from nuclear hydrodynamics:

$$k_\infty = \frac{3R^2 m}{h^2 \pi^2} [E_{(0^+)}]^2.$$

For an energy dependence of 80 $A^{-1/3}$ MeV as determined for the GMR (fig. 17) and $R = 1.2\ A^{1/3}$ fm, a value of $k_\infty \sim 200$ MeV is deduced. The GMR observation provides the first measure of the compressibility of nuclear matter, a fundamental nuclear property. The knowledge of the nuclear compressibility is important to such diverse applications as the formation of shock waves in heavy-ion reactions and the creation of neutron stars in the supernova process.

VI. Higher Multipole Resonances

The basic experimental question pertaining to high-L (≥ 3) giant resonances is whether the resonance strength is sufficiently localized in energy to be observable above the large nuclear continuum. Of course, similar questions were asked about the GQR before its observation. Nevertheless, there are good reasons, as discussed below, to expect that high-L resonances will be very difficult to observe.

1) For $L \geq 4$ the sum rule strength should be divided between at least three distinct classes of transitions. As shown on fig. 4, E4 excitations should be found at $0\hbar\omega$, $2\hbar\omega$ and $4\hbar\omega$. Thus, 100% of the EWSR is in this case distributed among three transition classes rather than two as is the case for the GQR.

2) The excitation energy expected for the high-L resonances is much higher than that of, for example, the GQR. That is to say, the $3\hbar\omega$ L=3, T=0, excitation should lie at a higher excitation energy than $2\hbar\omega$ excitation. Since the EWSR value is inversely proportional to the resonance energy, and the inelastic cross section is directly proportional to the EWSR, the

cross sections for the same EWSR depletion are lower for higher excitation states.

3) It is expected that the width of the giant resonances will increase as the excitation energy of the resonance (and the multipolarities of the resonance) increases. For example, calculations[12] by Nix and Sierk indicate that the width of the L=3 resonance should be ~ 3 times wider than the GQR while a L=4 resonance should be ~ 6 times broader than the GQR.

From these simple considerations one sees that searches for high-L giant resonances are faced with a decreased EWSR strength spread over a much wider excitation energy range than for low-L resonances.

The difficulties described above to observation of high-L giant resonances indicate the need for reactions which provide larger resonance cross sections and clear multipole identification through definitive angular distribution shapes. While no single reaction has appeared that will provide both of these desired features, the use of medium energy proton inelastic scattering provides excellent multipole selectivity and medium energy ($E \gtrsim 25$ MeV/amu) heavy ion inelastic scattering provides very large resonance cross sections. The use of heavy ions in giant resonance research is just beginning and will be discussed later in this presentation. However, use of medium energy proton inelastic scattering has already made significant contributions to the giant resonance field.

The most important advantages to medium energy (p,p') studies of giant resonances are shown in fig. 18 which shows a plot of calculated angular distributions for the reaction ^{208}Pb(p,p') at 200 MeV. Unlike

the case for lower energy protons and comparable energy alphas, large differences exist between the angular distributions of neighboring L-transfer values. For example, the difference between the angular distribution for a pure L=2 giant resonance and a mixed L=2+4 even for only 15-20% L=4 (EWSR) is very large. In addition, the cross sections are considerably larger in the angular distribution maximum than for the same L-transfer using lower energy protons. An additional advantage lies in the fact that the L=1 (isovector GDR) excitation proceeds overwhelmingly by Coulomb excitation which decreases rapidly with increasing angle. For angles greater tha ~ 5 degrees the GDR cross section is predicted to be as much as thirty times smaller than the L=0 cross section which occurs at the same excitation energy.

A. Isoscalar Giant Octupole Resonances

As discussed earlier there are two classes of octupole transitions, the $1\hbar\omega$ and $3\hbar\omega$ classes. In addition, the low-lying collective 3^- states generally account for very little of the T=0, E3 EWSR thus raising the possibility that considerable octupole strength may be found in the $3\hbar\omega$ transitions.

Recently, what has been interpreted as a localization of $1\hbar\omega$, 3^- strength has been observed[24] by inelastic scattering of alpha particles from a large number of nuclei. Results from these measurements are shown on fig. 19. For most nuclei a broad peak is observed at the systematic energy of ~ 32 $A^{-1/3}$ MeV. Although for ^{197}Au the peak falls considerably below this energy. Angular distributions for the peak cross section above the dashed line indicates an L=3 assignment for the

excitation. Suggestions of such strength were also made through the $^{197}Au(p,p')$ reaction[25] and the $^{116}Sn(e,e')$ reaction.[26] The fraction of the EWSR depleted in the so-called low-energy octupole resonance is 10-20% for most of the nuclei studied. No LEOR is observed in ^{40}Ca or ^{208}Pb.

Within the past year systematic observation of a $3\hbar\omega$ giant octupole resonance (GOR) have been made through inelastic scattering of 800-MeV protons,[27] 172-MeV alpha-particles,[28] and 110-140 MeV helium-3 particles[29] and 200 MeV protons.[30] Figure 20 shows spectra[30] from the reactions $^{90}Zr(p,p')$ and $^{120}Sn(p,p')$ for 200-MeV protons. Data are shown at angles which should provide maximum cross sections for excitation of the GDR, GQR and GCR.

At 4°, a large peak is observed which is located at the excitation energy of the GDR. The solid curve shown on the 4° data is the GDR shape and energy from (γ,n) measurements,[4] with magnitude fitted to our data. The GDR accounts for virtually the entire observed peak at 4°. The GMR is located at nearly the same energy as the GDR but the DWBA calculations (e.g., fig. 18) indicate that the GMR cross section is at least an order of magnitude smaller than that of the GDR at 4°. Since the E1 cross section drops rapidly with increasing angle, the E0 cross section becomes increasingly more important at larger angles. The 8° and 10° spectra were obtained at a maximum for the L=2 angular distribution for ^{90}Zr and ^{120}Sn, respectively. The solid curve, taken from the shape and location of the GQR as determined from (α,α') measurements,[8] provides excellent agreement with the present data. The cross section

for the GDR at the larger angles is greatly reduced from that observed at 4°. It can be assumed that at these angles, the cross section in the excitation energy region where GDR located is comprised of GDR and GMR components in unestablished proportions. In the 12° spectra broad peaks seen somewhat less clearly at 8° and 10° are observed at 25 ± 1 and 27 ± 1 MeV in ^{120}Sn and ^{90}Zr, respectively. Figure 21 shows angular distributions for these peaks. The data are seen to be very well described by the L=3 DWBA calculation but not at all by the L=4 calculation. Thus, we interpret these peaks as arising from excitation of the $3\hbar\omega$, GOR (E3).

Similar data were obtained[27] earlier from inelastic scattering of 800 MeV protons. Angular distributions from these data are shown in fig. 22. The data agree with the very characteristic angular distribution calculated for L=3. Figure 23 shows a spectrum from the $^{208}Pb(\alpha,\alpha')$ reaction[28] using 172-MeV alpha-particles. In addition to the GQR at 10.9 MeV and the GMR at 13.8 MeV the data indicate another peak which the authors subdivide into a peak at 17.5 MeV and one at 21.3 MeV. The angular distribution for the 17.5 MeV peak agrees very well with an L=3 DWBA calculation. (The authors assign the 21.3 MeV peak as an isoscalar dipole resonance [L=1,T=0,S=0].) The inelastic helium-3 measurements[29] were made on a wider mass range of nuclei and the angular distributions of the peaks are again well described by L=3.

The results from these measurements are summarized on fig. 24. The resonance excitation energy follows the systematic trend of $\sim 110\ A^{-1/3}$ MeV. The dashed line gives the value of $108.2\ A^{-1/3}$ MeV calculated in

ref. 12. The resonance width again follows the familiar trend of increasing width with decreasing nuclear mass. The dashed curve for the value 140 $A^{-2/3}$ is from ref. 12 where the constant has been adjusted from the author's suggested value in order to fit the experimental results. There is clear discrepancy in the sum rule depletion as deduced from the (α,α') and $(^3He,^3He')$ results on the one hand and the (p,p') results on the other hand. The EWSR strength depleted in giant resonances is inherently difficult to extract from inelastic hadron measurements because uncertainties in both the continuum shape and the model dependent calculations must be contended with. If one accepts, for example, the EWSR value for the T=0 GOR of ~ 60% for ^{208}Pb from the (α,α') measurement then all of the T=0 E3 sum rule strength is accounted for since ~ 45% of the strength lies in low lying states.[31]

These results suggest that the GOR ($3\hbar\omega$) has been located. However, as was the case ten years ago for the GQR and three years ago for the GMR, more data are needed to firmly establish the identity and systematics of this resonance.

B. Isoscalar Hexadecapole Giant Resonance

There has been no direct, (i.e. - peak observed in a spectrum), experimental evidence for an E4 giant resonance (4,0,0). RPA calculations for ^{208}Pb have shown[32] that the $2\hbar\omega$ giant hexadecapole resonance (GHR) should occur at virtually the same excitation energy as the $2\hbar\omega$ GQR. Other calculations[33] on ^{208}Pb indicate that ~ 40% of the L=4 EWSR should be located in the $2\hbar\omega$ transitions and ~ 60% in the $4\hbar\omega$ transitions. It was shown[34] through microscopic DWBA calculations

that the resonance cross sections from 61 MeV (p,p') and 96 MeV (α,α') measurements on ^{208}Pb were consistent with the existence of ~ 20% of the T=0 E4 EWSR within the (predominately) GQR peak. However, the inclusion of L=4 strength was based only on the total resonance cross section since the angular distributions could not definitively indicate a necessity for inclusion of GHR strength.

While the angular distributions for L=2 and L=4 excitations are not very different in low energy proton and alpha-particle inelastic scattering, as pointed out earlier, the differences are very large for higher energy inelastic proton scattering. The angular distribution differences between L=2 and L=4 should provide for rather easy detection of a 20-40% mixture of E4 strength in the GQR peak even with uncertainties on the data as large as 20-30%.

Figure 25 shows angular distributions[30] for the GQR peak from the reaction $^{90}Zr(p,p')$ and $^{120}Sn(p,p')$ (fig. 20). The comparisons of fig. 25 show that the GQR cross sections are well described by the L=2 DWBA calculation. The sensitivity of these results to higher multipole contributions in the GQR peak is shown by the dashed curve which results from a mixture of only 5% of the L=4, EWSR, with the L=2 angular distribution. Clearly, the GQR peak contains very little, if any, contribution from excitation of a $2\hbar\omega$, E4, giant resonance. This statement only indicates that there is no major L=4 strength within the GQR peaks shown in fig. 20. Strength from $2\hbar\omega$, E4, resonance excitation may be present but, may be many MeV wide and thus, escape detection in the present experiment. Similar results have been obtained for ^{60}Ni and ^{208}Pb.

The location of the GHR is thus an unsolved question. If the strength is localized at all it will probably be situated at very high excitation energies. The calculations of ref. 12 place the L=4 strength at 150 $A^{-1/3}$ MeV or ~ 25 MeV in ^{208}Pb. It is also very likely that the peak would be even broader than that reported for the GOR. Location of the GHR presents a considerable experimental challenge as does the location of even higher multipole resonances.

VII. Future Directions

There are many uses of direct reactions for giant resonance studies that I have not described. Of these, the recent work in charge exchange studies of isospin/spin flip giant resonances is most notable. Such studies as (p,n), (n,p) and ($\pi^{\pm}$, π°) require another lecture in order to do justice to the topic. I believe the recent results from these charge exchange measurements are only the beginning of a very exciting new era of measurement in giant resonances.

Since this discussion has dealt nearly exclusively with excitation of the so-called new giant resonances via inelastic scattering of medium energy hadrons, I would like to mention two inelastic reactions which show potential promise for giant resonance studies, but which have not yet been exploited. Some of the future direction in this field is certainly to be found in the use of heavy-ion inelastic scattering and pion inelastic scattering. I briefly discuss some very new results from the heavy-ion field.

The primary advantage to heavy-ion excitation of giant resonances is the large resonance cross section expected with higher energy incident beams. Figure 26 is a plot of maximum cross section (grazing

angle) versus incident energy for L=2 and L=4 excitation (Q = -12 MeV, 100% EWSR) in the reaction $^{208}Pb(^{16}O,^{16}O')$. For 400 MeV ^{16}O beams the GQR cross section should be ~ 50 mb/sr, nearly five times larger than for the 200 MeV (p,p') reaction and twice as large as achieved with 150 MeV alpha-particle inelastic scattering. Some measurements of giant resonance excitation using low-energy heavy-ions have been made.[35] However, the small cross sections realized in those measurements provides no advantage, in fact, provides a disadvantage over what can be achieved with other probes.

Recently, measurements[36] have been made of inelastic excitation of giant resonances using the 400 MeV ^{16}O beam from the HHIRF accelerator at Oak Ridge National Laboratory. A partial spectrum of the giant resonances is shown on fig. 27. The GQR is clearly visible at 10.9 MeV as is a peak at 13.7 MeV which arises from excitation of the GMR and GQR. The peak at 17.6 MeV is not completely understood but may be the same as the peak reported[28] to be L=3 in 172 MeV alpha-inelastic scattering (fig. 23). The peak at 24.8 MeV probably arises from kinematical nucleon pick-up and subsequent decay processes. The large peak (off scale) at ~ 7 MeV of excitation arises from excitation of states in the ^{16}O projectile which are Doppler broadened. The solid lines indicate fits to the peaks and the estimation of the shape and magnitude of the underlying continuum.

The most obvious giant resonance feature in the spectrum of fig. 27 is the very large ratio of the GQR peak height to the height of the underlying continuum. The ratio is ~ 2.2:1. Using 152-MeV alpha particles[8] the best ratio obtained for the GQR in ^{208}Pb is ~ 1:1.

The measured angular distributions for the GQR and GDR + GMR peaks are shown on fig. 28. Indeed the GQR cross section reaches a value of 50 mb/sr over twice that obtained using 150 MeV incident alphas. The calculations show that ~ 100% of the GQR is accounted for, in excellent agreement with results using other probes. However, the calculations assuming 100% of the GMR cannot, by nearly a factor of three at small angles, account for the magnitude of the 13.7 MeV peak. Since the ^{16}O projectile is isoscalar it is expected that nuclear excitation of the GDR would be very small. Coulomb excitation of the GDR is indeed possible and the calculated GDR cross section is shown on fig. 28. However, the sum of the GDR and GMR excitations do not quite agree with the data. It is to be noted that there is no low-lying GMR state in which to test the calculation.

Thus, use of heavy-ion inelastic scattering does indeed, provide a very large GQR cross section with the added benefit of a very large peak to continuum ratio. This combination makes the heavy-ion probe very useful for excitation of the GQR and measurement of the resonance subsequent decay modes, especially rare decay modes.

VIII. Summary

Through this rather rapid summarization of the experimental measurements of electric giant multipole resonances hopefully one sees that the field has progressed a great deal during the past ten years. The parameters of the giant quadrupole resonance are now firmly established by an extensive set of measurements. The GQR is providing a significant influence in other areas of nuclear physics. The monopole resonance has now been established

and its observation has provided the first direct measure of the nuclear compressibility. A strong case for the existence of a giant octupole resonance is now being made through a variety of hadron reactions.

However, we certainly have not exhausted the supply of giant multipole resonances. The newer techniques such as higher energy proton scattering, charge exchange reactions, heavy-ion scattering and pion reactions offer considerable hope for identifying new resonances during the next few years. We have come a long way in the past ten years but there is still a great deal to do in the giant multipole resonance field.

References

1. References to work in this area prior to 1976 can be found in the following reference: Fred E. Bertrand, Annual Review of Nuclear Science 26, 457 (1976).
2. "Giant Multipole Resonances," Proceedings of the Giant Multipole Resonance Topical Conference, Oak Ridge, Tennessee, October 1979, ed. Fred E. Bertrand (Harwood Academic Publishers, New York, 1980).
3. Fred E. Bertrand, Nucl. Phys. A354, 129c (1981).
4. For a review of the giant dipole resonance see: B. L. Berman and S. C. Faltz, Rev. Mod. Phys. 47, 713 (1975).
5. G. R. Satchler, Nucl. Phys. A195, 1 (1972). G. R. Satchler, Part. Nuclei 5, 105 (1973).
6. B. R. Mottelson, Proceedings of Solvay Conference of Physics, 15th, Brussels, 1970, ed. I. Pregogine (Gordon and Breach, New York).
7. F. E. Bertrand and R. W. Peelle, Phys. Rev. C 8, 1045 (1973).
8. F. E. Bertrand, G. R. Satchler, D. J. Horen, J. R. Wu, A. D. Bacher, G. T. Emery, W. P. Jones, D. W. Miller and A. van der Woude, to Phys. Rev. C 22, 1832 (1980).
9. K. van der Borg, Thesis, 1979, Groningen University, The Netherlands (unpublished).
10. K. van der Borg, M. N. Harakeh, S. Y. van der Werf, A. van der Woude and F. E. Bertrand, Phys. Lett. 67B, 405 (1977).
11. F. E. Bertrand, K. van der Borg, A. G. Drentje, M. N. Harakeh, J. van der Plicht and A. van der Woude, Phys. Rev. Lett. 40, 635 (1978).
12. J. Rayford Nix and Arnold J. Sierk, Phys. Rev. C 21, 396 (1980).

13. F. P. Brady, N.S.P. King, M. W. McNaughton and G. R. Satchler, Phys. Rev. Lett. 36, 15 (1976). See also review articles by F. Paul Brady and G. A. Needham; N.S.P. King and J. L. Ullmann in "The (p,n) Reaction and the Nucleon-Nucleon Force," proceedings, Telluride, Colorado (1979).

14. R. Pitthan, G. M. Bates, J. S. Beachy, E. B. Dally, D. H. Dubois, J. N. Dyer, S. J. Kowalick and F. R. Buskirk, Phys. Rev. C 21, 147 (1980).

15. Rainer Pitthan, in "Giant Multipole Resonances," Proceedings of the Giant Multipole Resonance Topical Conference, Oak Ridge, Tennessee, October 1979, ed. Fred E. Bertrand (Harwood Academic Publishers, New York, 1980), p. 161.

16. N. Marty, M. Morlet, H. Willis, V. Comparat, R. Frascaria and J. Kallne, Institute of Nuclear Physics, Orsay, Report No. IPNO-PH-N-75-11 (1975), unpublished.

17. S. Fukuda and Y. Torizuka, Phys. Lett 62B, 146 (1976); M. Sasao and Y. Torizuka, Phys. Rev. C 15, 217 (1977).

18. M. N. Harakeh, K. van der Borg, T. Ishimatsu, H. P. Morsch, A. van der Woude and F. E. Bertrand, Phys. Rev. Lett. 38, 676 (1977).

19. D. H. Youngblood, C. M. Rozsa, J. M. Moss, D. R. Brown and J. D. Bronson, Phys. Rev. Lett. 39, 1188 (1977).

20. M. Buenerd, C. Bonhomme, D. Lebrun, P. Martin, J. Chauvin, G. Duhanel, G. Perrin, P. de Saintignon, Phys. Lett. 84B, 305 (1979).

21. D. H. Youngblood, in "Giant Multipole Resonances," Proceedings of the Giant Multipole Resonance Topical Conference, Oak Ridge, Tennessee, October 1979, ed. Fred E. Bertrand (Harwood Academic Publishers, New York, 1980), p. 113.

22. C. M. Rozsa, D. H. Youngblood, J. D. Bronson, Y.-W. Lui and U. Garg, Phys. Rev. C 21, 1252 (1980).

23. F. E. Bertrand, G. R. Satchler, D. J. Horen and A. van der Woude, Phys. Lett. 80B, 198 (1979); F. E. Bertrand, G. R. Satchler, D. J. Horen and A. van der Woude, Phys. Rev. C 18, 2788 (1978).

24. J. M. Moss, D. H. Youngblood, C. M. Rozsa, D. R. Brown and J. D. Bronson, Phys. Rev. Lett 37, 816 (1976); J. M. Moss, D. R. Brown, D. H. Youngblood, C. M. Rozsa and J. D. Bronson, Phys. Rev. C 18, 741 (1978).

25. F. E. Bertrand and D. C. Kocher, Phys. Rev. C 13, 2241 (1976).

26. K. Hosoyama and Y. Torizuka, Phys. Rev. Lett. 35, 199 (1975).

27. T. A. Carey, W. D. Cornelius, N. J. DiGiacomo, J. M. Moss, G. S. Adams, J. B. McClelland, G. Pauletta, C. Whitten, M. Gozzaly, N. Hintz and C. Glashausser, Phys. Rev. Lett. 45, 239 (1980).

28. H. P. Morsch, M. Rogge, P. Turek and C. Mayer-Böricke, Phys. Rev. Lett. 45, 337 (1980).

29. T. Yamagata, S. Kishimoto, K. Yuasa, K. Iwamoto, B. Saeki, M. Tanaka, T. Fukuda, I. Miura, H. Inoue and H. Ogato, submitted for publication.

30. F. E. Bertrand, E. E. Gross, D. J. Horen, J. R. Wu, J. T. Tinsley, D. K. McDaniels, L. W. Swenson and R. Liljestrand, Phys. Lett. 103B, 326 (1981); and unpublished results, same authors.

31. M. B. Lewis, F. E. Bertrand and C. B. Fulmer, Phys. Rev. C 7, 1966 (1973).

32. P. Ring and J. Speth, Phys. Lett. B44, 477 (1973); P. Ring and J. Speth, Nucl. Phys. A235, 315 (1974).

33. I. Hamamoto, Nucl. Phys. A196, 101 (1972).

34. E. C. Halbert, J. B. McGrory, G. R. Satchler and J. Speth, Nucl. Phys. A245, 189 (1975).

35. For summary of these early results see: A. van der Woude, in "Giant Multipole Resonances," Proceedings of the Giant Multipole Resonance Topical Conference, Oak Ridge, Tennessee, October 1979, ed. Fred E. Bertrand (Harwood Academic Publishers, New York, 1980), p. 65.

36. T. P. Sjoreen, F. E. Bertrand, R. L. Auble, K. A. Erb, E. E. Gross, D. J. Horen and D. Shapira, unpublished data.

Figure Captions

Fig. 1. Giant dipole resonance in ^{208}Pb as observed in the (γ,n) reaction (ref. 4).

Fig. 2. Systematics of the isovector giant dipole resonance excitation energy, width and sum rule depletion (ref. 4).

Fig. 3. Modes of oscillation of a nucleus.

Fig. 4. Schematic representation of electric multipole transitions between shell-model states of a hypothetical nucleus. Major shells are denoted as N, N+1, N+2, etc. and lie $\sim 1\hbar\omega$ or $\sim 41 \times A^{-1/3}$ MeV apart.

Fig. 5. Percent energy weighted sum rule depleted in the first excited 2^+ state plotted versus Z and N.

Fig. 6. Proton spectrum at 27° from 62 MeV protons in ^{54}Fe. The energy of the outgoing proton is plotted at the bottom of the figure, while the approximate excitation energy is plotted at the top. Data have been plotted in ~ 1 MeV-wide bins up to ~ 49 MeV, then plotted in 50 keV-wide bins. Protons below ~ 1.5 MeV were not detected in the experiment. The small, broad peak near $E_x \sim 16$ MeV is identified as arising from excitation of the giant quadrupole and dipole resonances (ref. 7).

Fig. 7. $^{120}Sn(\alpha,\alpha')$ spectra for $E_\alpha = 152$ MeV (ref. 8). A decomposition of the spectrum into giant resonances (established and possible) and a continuum is shown on the 13 degree spectrum.

Fig. 8. Spectra from inelastic scattering of 152-MeV alpha-particles on ^{208}Pb, ^{120}Sn, ^{90}Zr, ^{58}Ni and ^{46}Ti. The giant resonance structure located near the excitation energy $63 \times A^{-1/3}$ MeV has been

decomposed into contributions from the giant quadrupole and giant monopole resonances. The peak located at higher excitation energy in the ^{208}Pb and ^{120}Sn spectra are due to hydrogen contamination of the target (ref. 8).

Fig. 9. Angular distributions of the E2 portion of the spectra from fig. 6. The data are compared to an L=2 DWBA calculation normalized to the indicated EWSR depletions (ref. 8).

Fig. 10. (α,α') spectra for 120 MeV alphas on ^{24}Mg, ^{26}Mg, ^{28}Si and ^{40}Ca (ref. 9). The arrows are located at the excitation energy $63 \times A^{-1/3}$ MeV.

Fig. 11. Systematics for the excitation energy, width and sum rule depletion of the isoscalar giant quadrupole resonance. The data are mostly from refs. 1 and 2.

Fig. 12. Left; Inelastic electron scattering from ^{60}Ni. The broad peak at ~ 32 MeV of excitation is assigned as isovector quadrupole resonance (ref. 14). Right; Form factors for the isovector E2 states observed (ref. 14) in ^{58}Ni and ^{60}Ni. The solid curve is for the Goldhaber-Teller model while the dashed curve is from the Myers-Swiatecki prescription.

Fig. 13. Systematics of the excitation energy, width and sum rule depletion of the isovector giant quadrupole resonance. The data are from ref. 15.

Fig. 14. Calculated inelastic scattering angular distributions for 152 MeV alpha particle excitation of the GQR and GMR in ^{208}Pb compared with data from ref. 8.

Fig. 15. Inelastic alpha particle spectra at very small angles for 129-MeV alpha-particles in ^{144}Sm and ^{154}Sm (ref. 21).

Fig. 16. Top; Giant resonance spectra from the reaction $^{116}Sn(\alpha,\alpha')$ for E_α = 129 MeV. The nuclear continuum has been subtracted from the data. The peak is decomposed into monopole and quadrupole contributions (ref. 22).

Fig. 17. Systematics for the excitation energy width and sum rule depletion for the isoscalar giant monopole resonance. Data are from refs. 19, 20, 21 and 23.

Fig. 18. DWBA calculations for excitation of various multipoles (all isoscalar except L=1 is isovector) by the reaction $^{208}Pb(p,p')$ for E_p = 200 MeV.

Fig. 19. Inelastic alpha-particle spectra from several nuclei bombarded by 96 and 115 MeV alpha-particles. The low-energy octupole resonance is located above the dashed line (ref. 24).

Fig. 20. Spectra from inelastic scattering of 200-MeV protons from ^{90}Zr and ^{120}Sn (ref. 30). The multipolarities shown for the resonances are discussed in the text. The dashed line shows the shape and magnitude assumed for the nuclear continuum underlying the rsonance peaks.

Fig. 21. Angular distributions for the GOR compared with DWBA calculations (solid and dashed curves) (ref. 30).

Fig. 22. Angular distributions for the giant octupole resonance as excited by 800-MeV protons (ref. 27).

Fig. 23. Giant resonance spectra from inelastic scattering of 172-MeV alpha particles from ^{208}Pb. The resonance structure is decomposed into a GQR (10.9 MeV), GMR (13.8 MeV), a proposed giant octupole resonance (17.5 MeV) and an isoscalar giant dipole resonance (21.3 MeV) (ref. 28).

Fig. 24. Systematics of the excitation energy width and sum rule depletion for the isoscalar octupole resonance as proposed from the indicated experiments (refs. 27, 28, 29 and 30).

Fig. 25. Angular distributions for the GQR peak in ^{90}Zr and ^{120}Sn excited via 200 MeV (p,p') compared with DWBA calculations (solid and dashed curves) (ref. 30).

Fig. 26. Grazing angle cross sections calculated for L=2 and L=4 excitations by the reaction $^{208}Pb(^{16}O,^{16}O')$ plotted as a function of incident ^{16}O energy (100% EWSR).

Fig. 27. Spectrum from the reaction $^{208}Pb(^{16}O,^{16}O')$ for $E_{^{16}O}$ = 400 MeV. The solid curves are fits to the peaks and an estimate of the shape and magnitude of the underlying continuum (ref. 36).

Fig. 28. Angular distributions for excitation of the GQR (10.9 MeV) and the GDR + GMR (13.7 MeV) peak. DWBA calculations for indicated L-transfers are shown as solid and dashed curves (ref. 36).

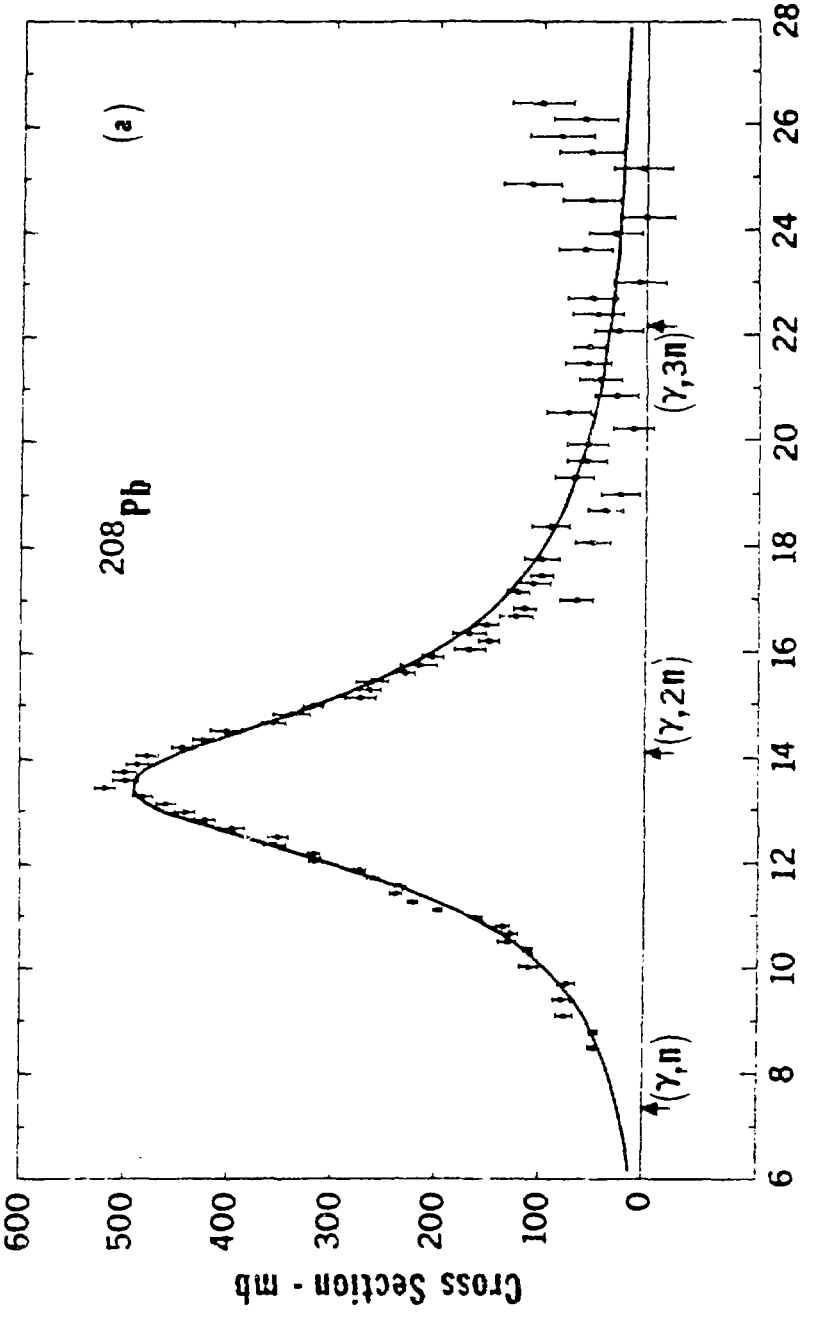
(a)
^{208}Pb
(γ,n)
(γ,2n)
(γ,3n)
Cross Section - mb
Photon Energy - MeV
0
100
200
300
400
500
600
6
8
10
12
14
16
18
20
22
24
26
28

Fig. 1

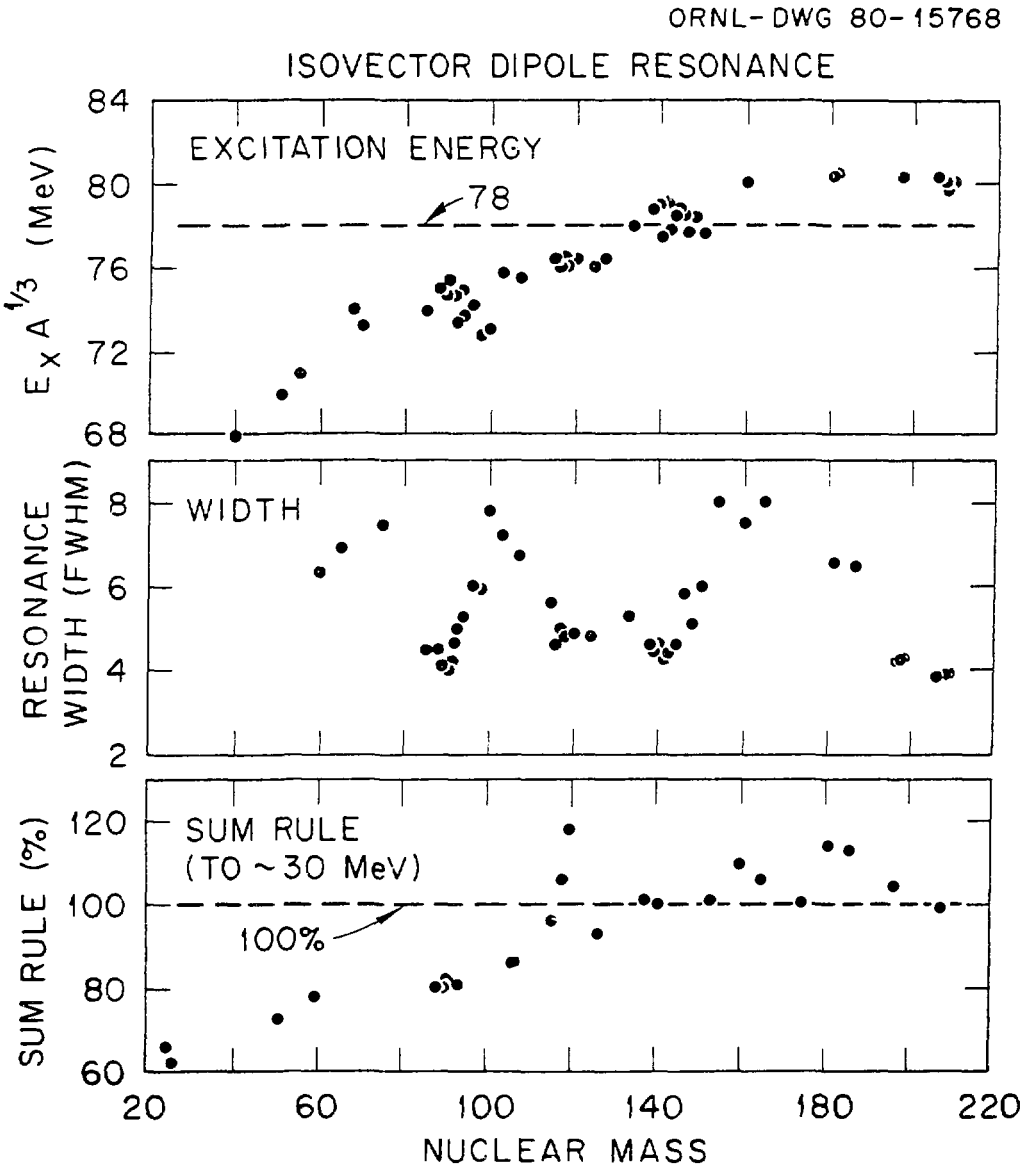
ORNL-DWG 80-15768
ISOVECTOR DIPOLE RESONANCE
EXCITATION ENERGY
78
$E_x A^{1/3}$ (MeV)
84
80
76
72
68
WIDTH
RESONANCE WIDTH (FWHM)
8
6
4
2
SUM RULE
(TO ~30 MeV)
100%
SUM RULE (%)
120
100
80
60
20
60
100
140
180
220
NUCLEAR MASS

Fig. 2

ORNL-DWG 80-15861

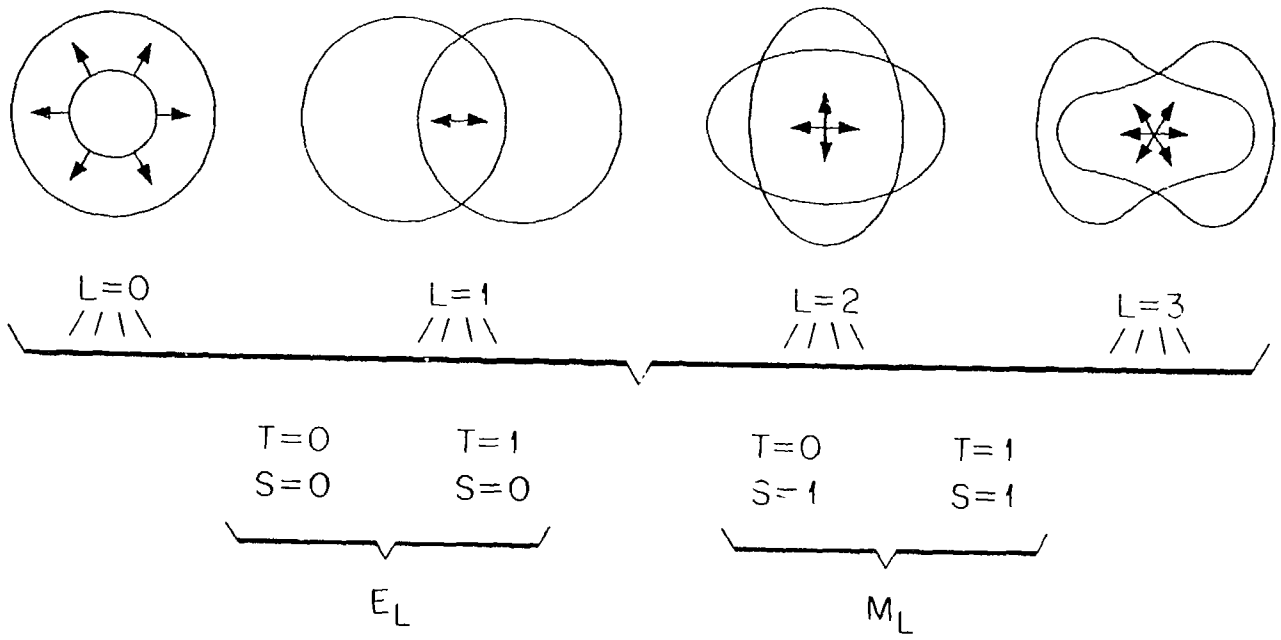

Fig. 3

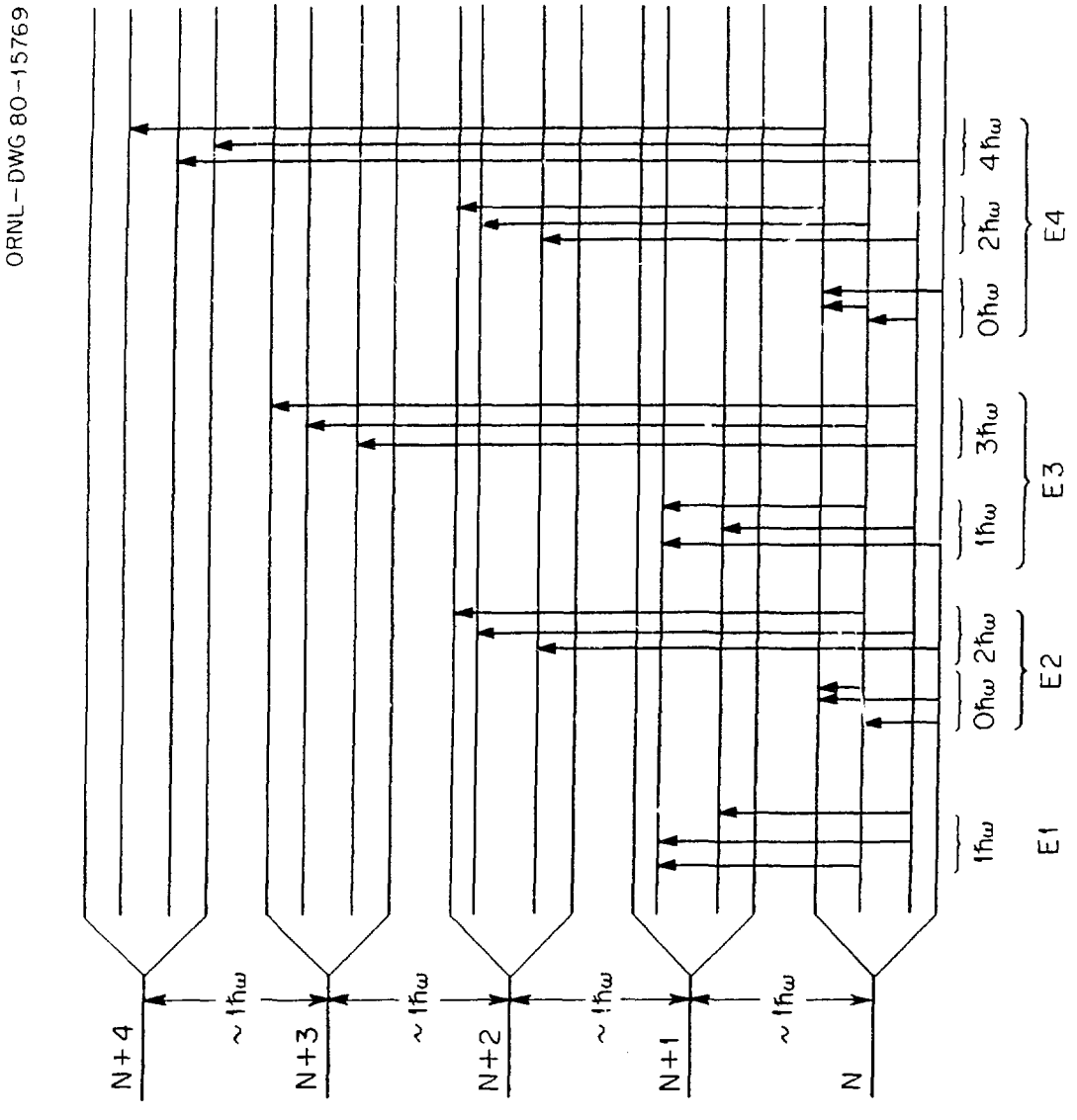
ORNL-DWG 80-15769
N+4
N+3
N+2
N+1
N
~1ħω
~1ħω
~1ħω
~1ħω
1ħω
0ħω 2ħω
1ħω 3ħω
0ħω 2ħω 4ħω
E1
E2
E3
E4

Fig. 4

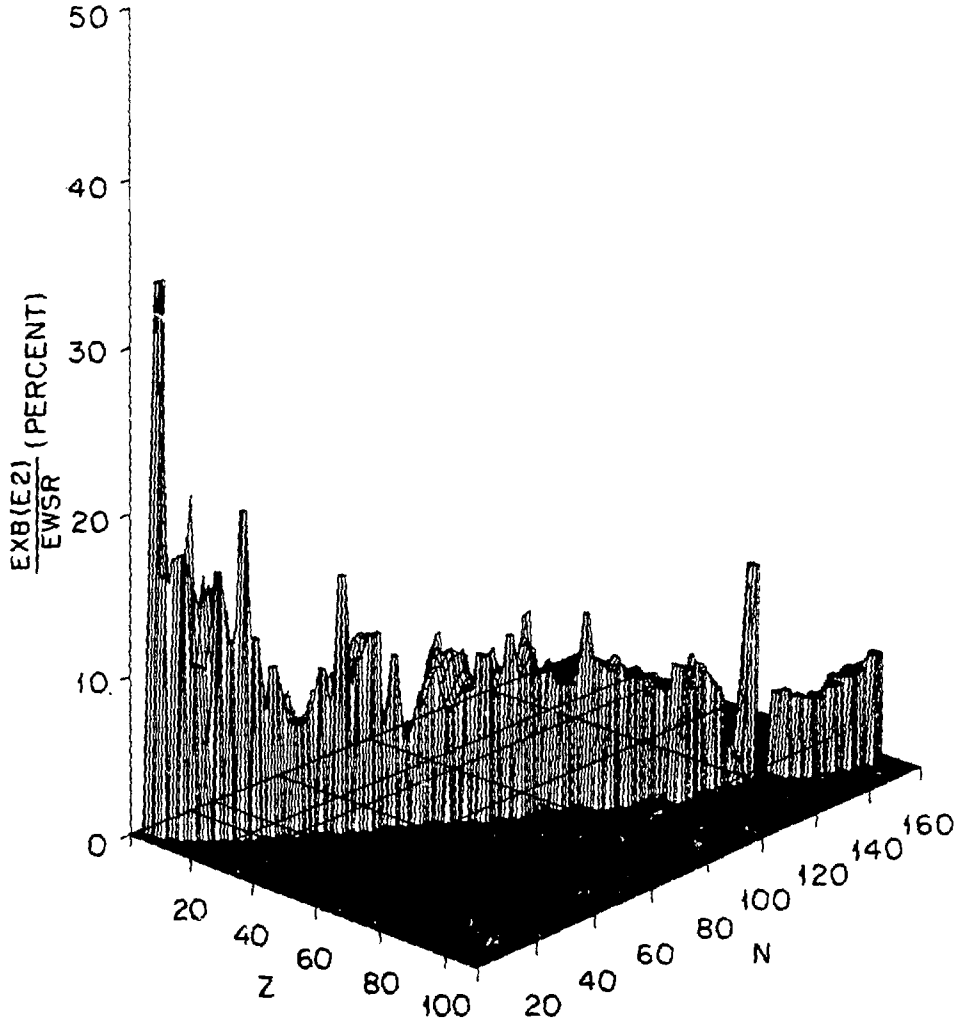
50
40
30
20
10
0
EXB(E2)/EWSR (PERCENT)
20
40
60
80
100
Z
20
40
60
80
100
120
140
160
N

Fig. 5

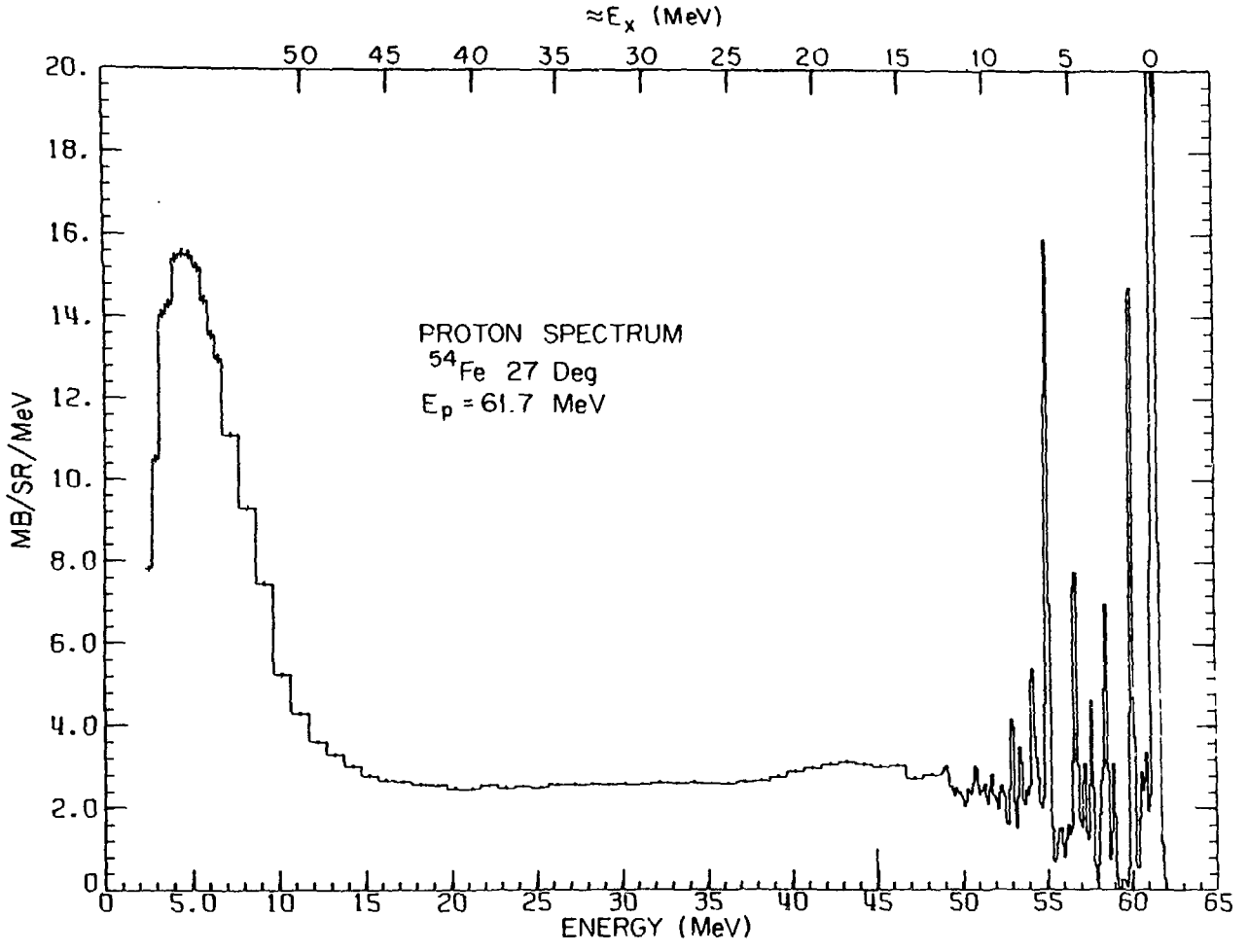
≈E_x (MeV)
50 45 40 35 30 25 20 15 10 5 0
PROTON SPECTRUM
54Fe 27 Deg
E_p = 61.7 MeV
MB/SR/MeV
ENERGY (MeV)
0 2.0 4.0 6.0 8.0 10. 12. 14. 16. 18. 20.
0 5.0 10 15 20 25 30 35 40 45 50 55 60 65

Fig. 6

ORNL-DWG 80-15706

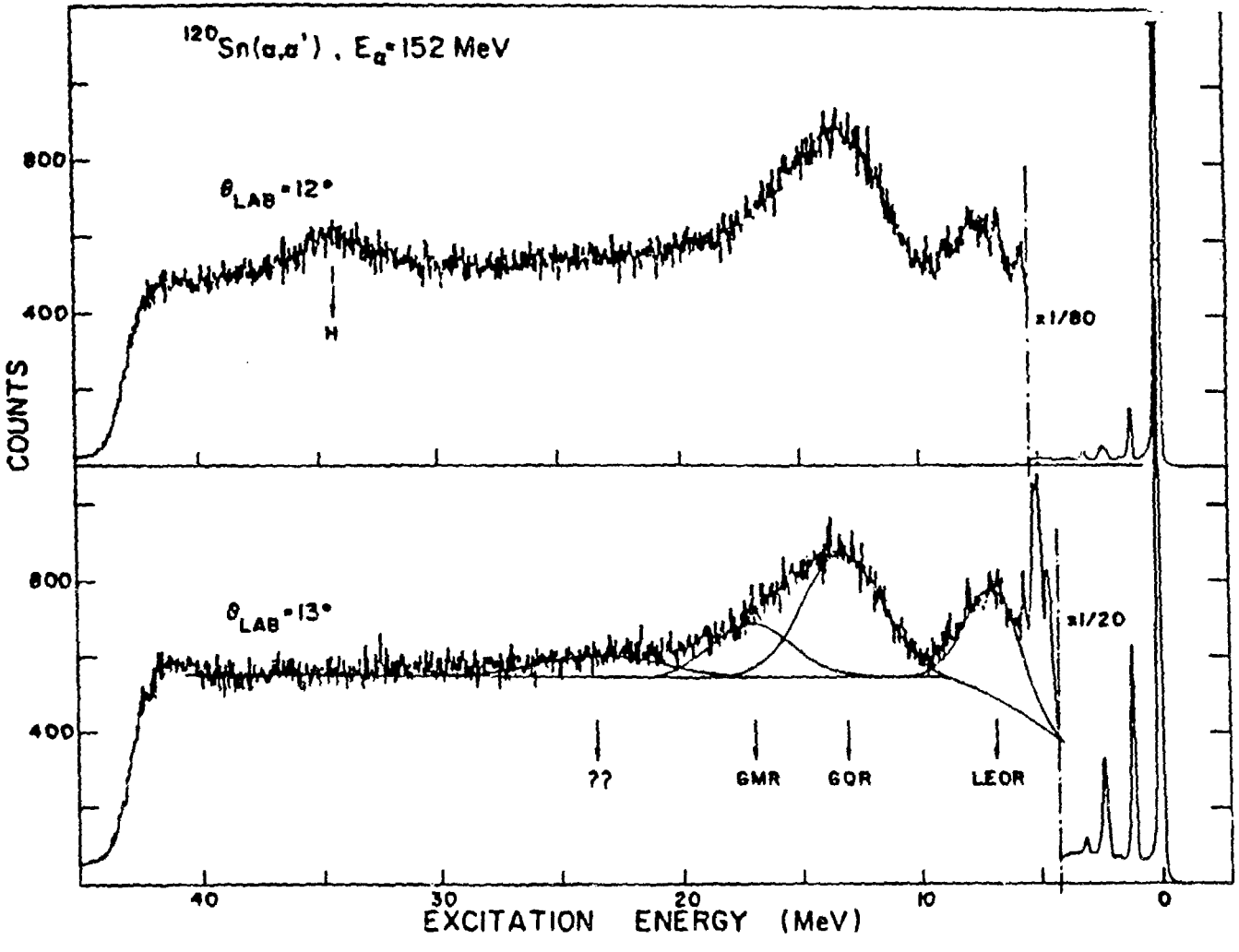

Fig. 7

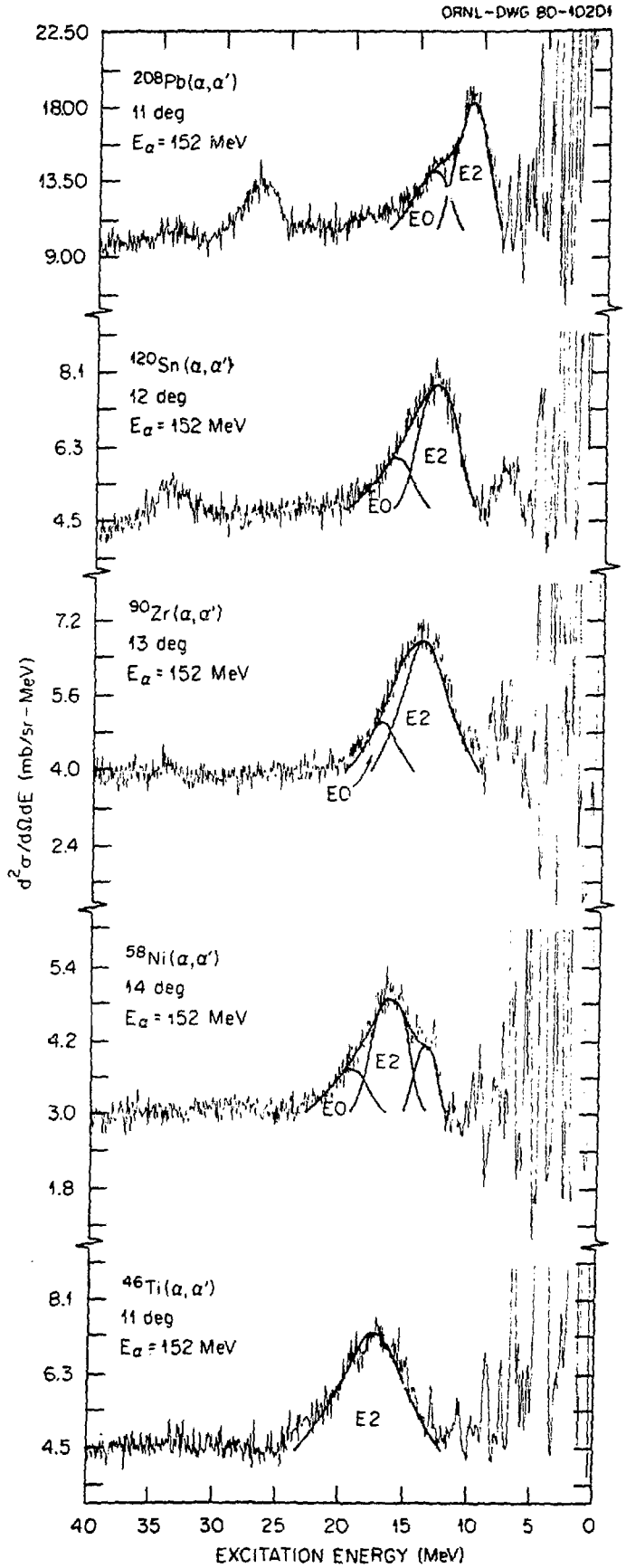
ORNL-DWG 80-10201
22.50
18.00
13.50
9.00
208Pb(α,α')
11 deg
Eα = 152 MeV
E2
E0
8.1
6.3
4.5
120Sn (α,α')
12 deg
Eα = 152 MeV
E2
E0
7.2
5.6
4.0
2.4
90Zr(α,α')
13 deg
Eα = 152 MeV
E2
E0
d²σ/dΩdE (mb/sr - MeV)
5.4
4.2
3.0
1.8
58Ni(α,α')
14 deg
Eα = 152 MeV
E2
E0
8.1
6.3
4.5
46Ti(α,α')
11 deg
Eα = 152 MeV
E2
40
35
30
25
20
15
10
5
0
EXCITATION ENERGY (MeV)

Fig. 8

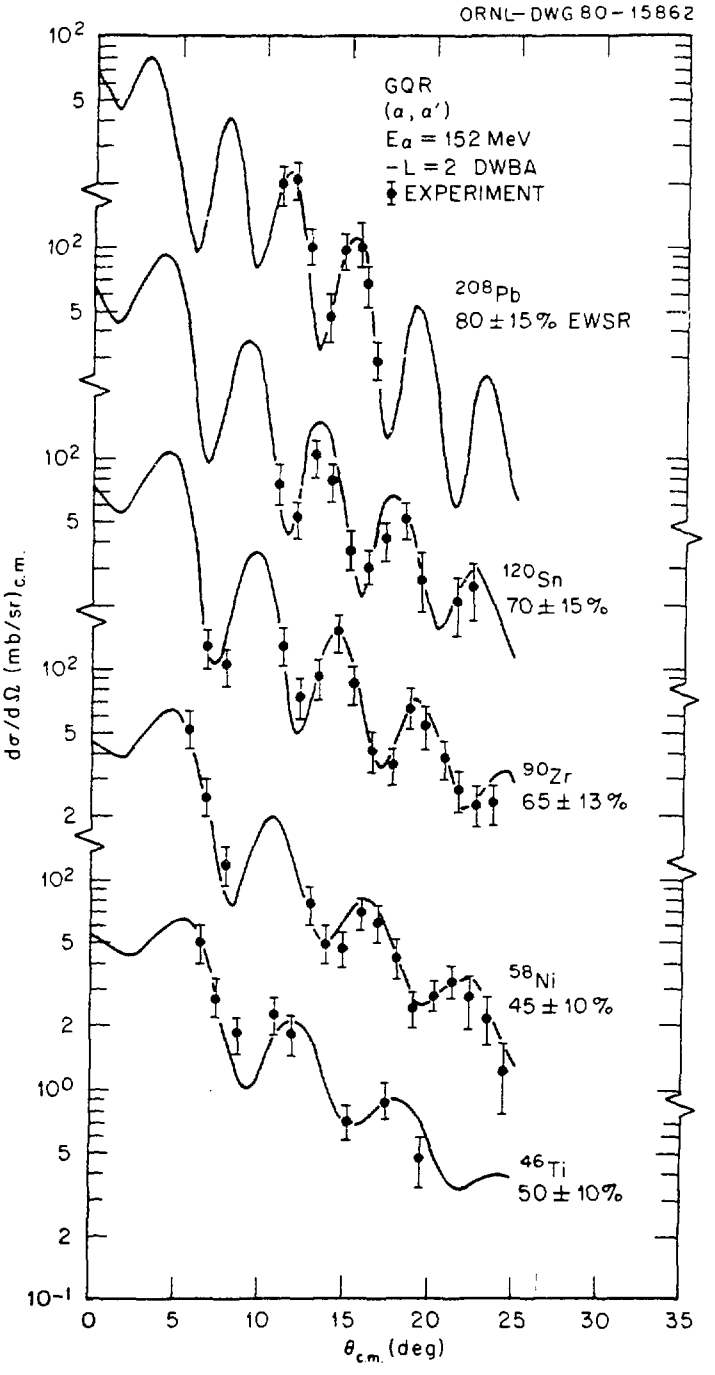
ORNL-DWG 80-15862
GQR
(a, a')
Ea = 152 MeV
-L=2 DWBA
EXPERIMENT
208Pb
80 ± 15% EWSR
120Sn
70 ± 15%
90Zr
65 ± 13%
58Ni
45 ± 10%
46Ti
50 ± 10%
dσ/dΩ (mb/sr)c.m.
θc.m. (deg)

Fig. 9

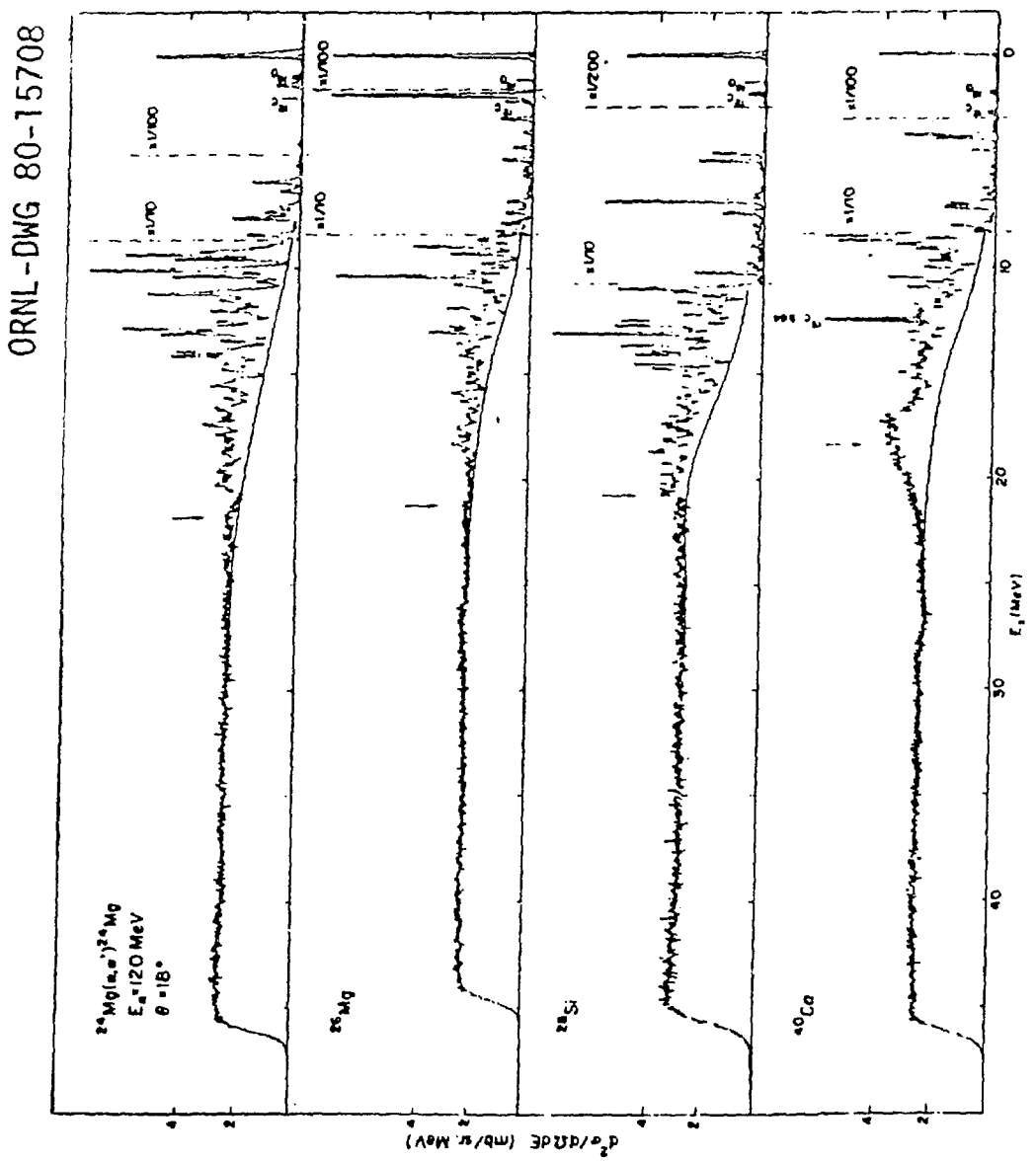
ORNL-DWG 80-15708
$^{24}Mg(\alpha,\alpha')^{24}Mg$
E_α=120 MeV
θ=18°
^{26}Mg
^{28}Si
^{40}Ca
1=1/10
1=1/100
1=1/1000
$d^2\sigma/d\Omega dE$ (mb/sr MeV)
E_x(MeV)

Fig. 10

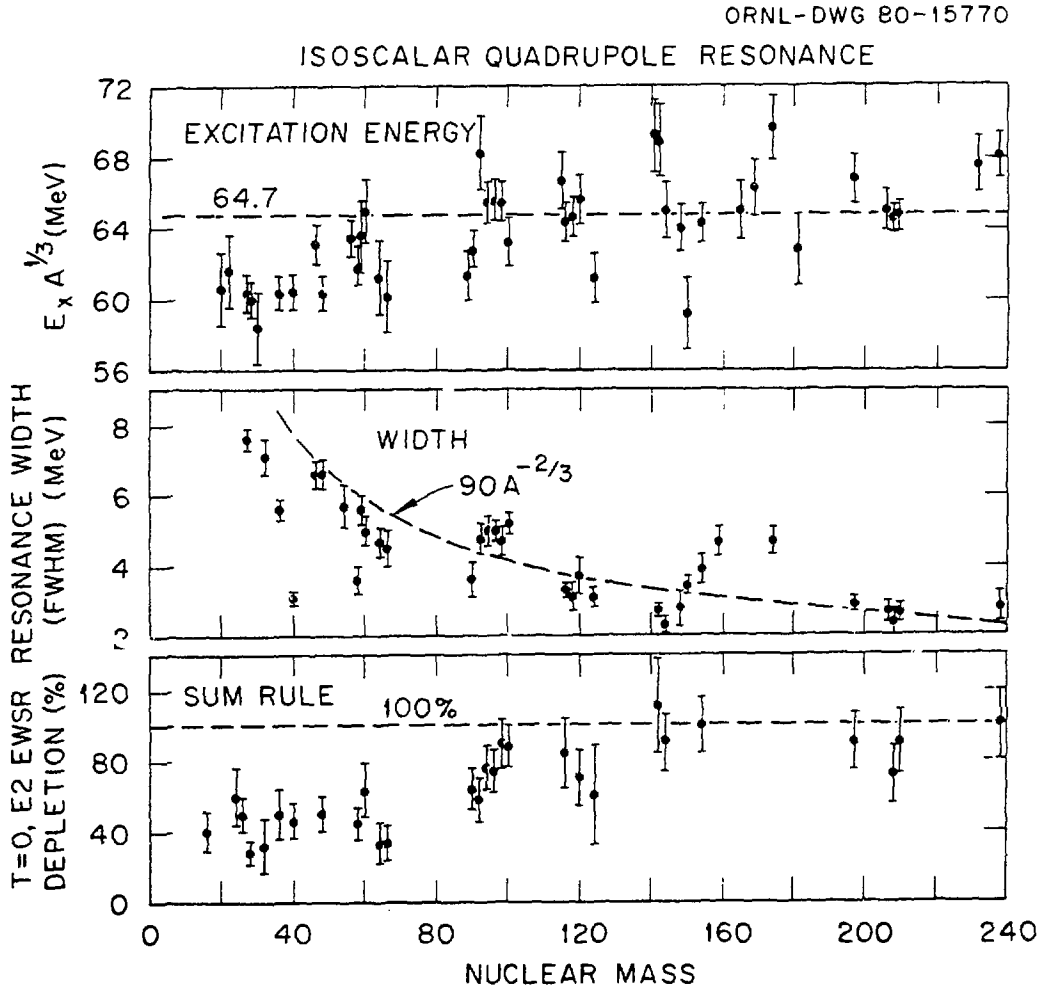
ORNL-DWG 80-15770
ISOSCALAR QUADRUPOLE RESONANCE
EXCITATION ENERGY
64.7
$E_x A^{1/3}$ (MeV)
WIDTH
$90 A^{-2/3}$
T=0, E2 EWSR RESONANCE WIDTH (FWHM) (MeV)
SUM RULE
100%
DEPLETION (%)
NUCLEAR MASS

Fig. 11

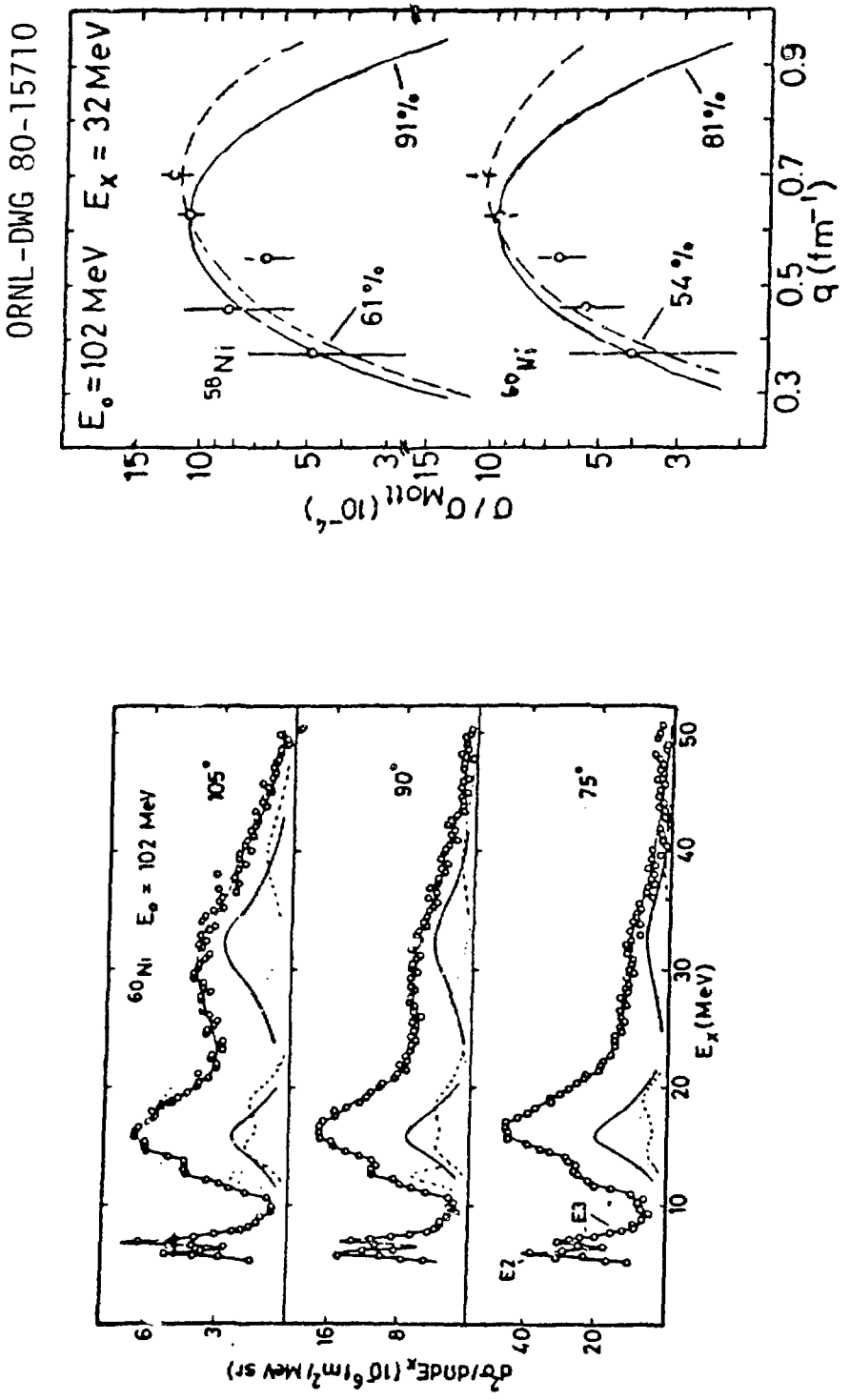
ORNL-DWG 80-15710
E_o = 102 MeV E_x = 32 MeV
^{58}Ni
^{60}Ni
61%
91%
54%
81%
σ / σ$_{Mott}$ (10^{-4})
q (fm^{-1})
^{60}Ni E_o = 102 MeV
105°
90°
75°
E2
E3
d^{2}σ/dΩdE$_x$ (10^{6}fm^2/MeV sr)
E$_x$ (MeV)

Fig. 12

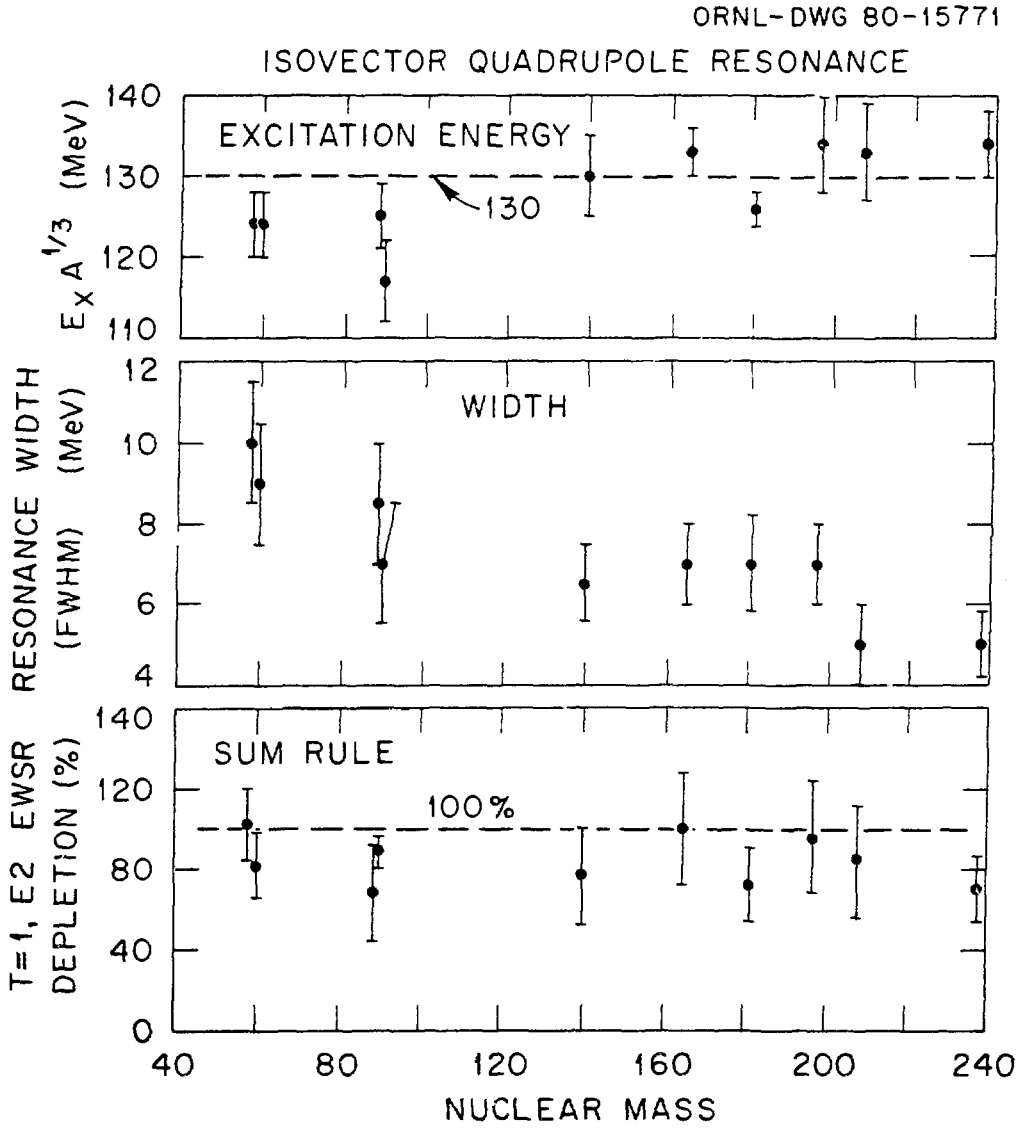
ORNL-DWG 80-15771
ISOVECTOR QUADRUPOLE RESONANCE
EXCITATION ENERGY
130
$E_x A^{1/3}$ (MeV)
140
130
120
110
WIDTH
RESONANCE WIDTH (FWHM) (MeV)
12
10
8
6
4
SUM RULE
100%
T=1, E2 EWSR DEPLETION (%)
140
120
80
40
0
40
80
120
160
200
240
NUCLEAR MASS

Fig. 13

ORNL-DWG 80-15860

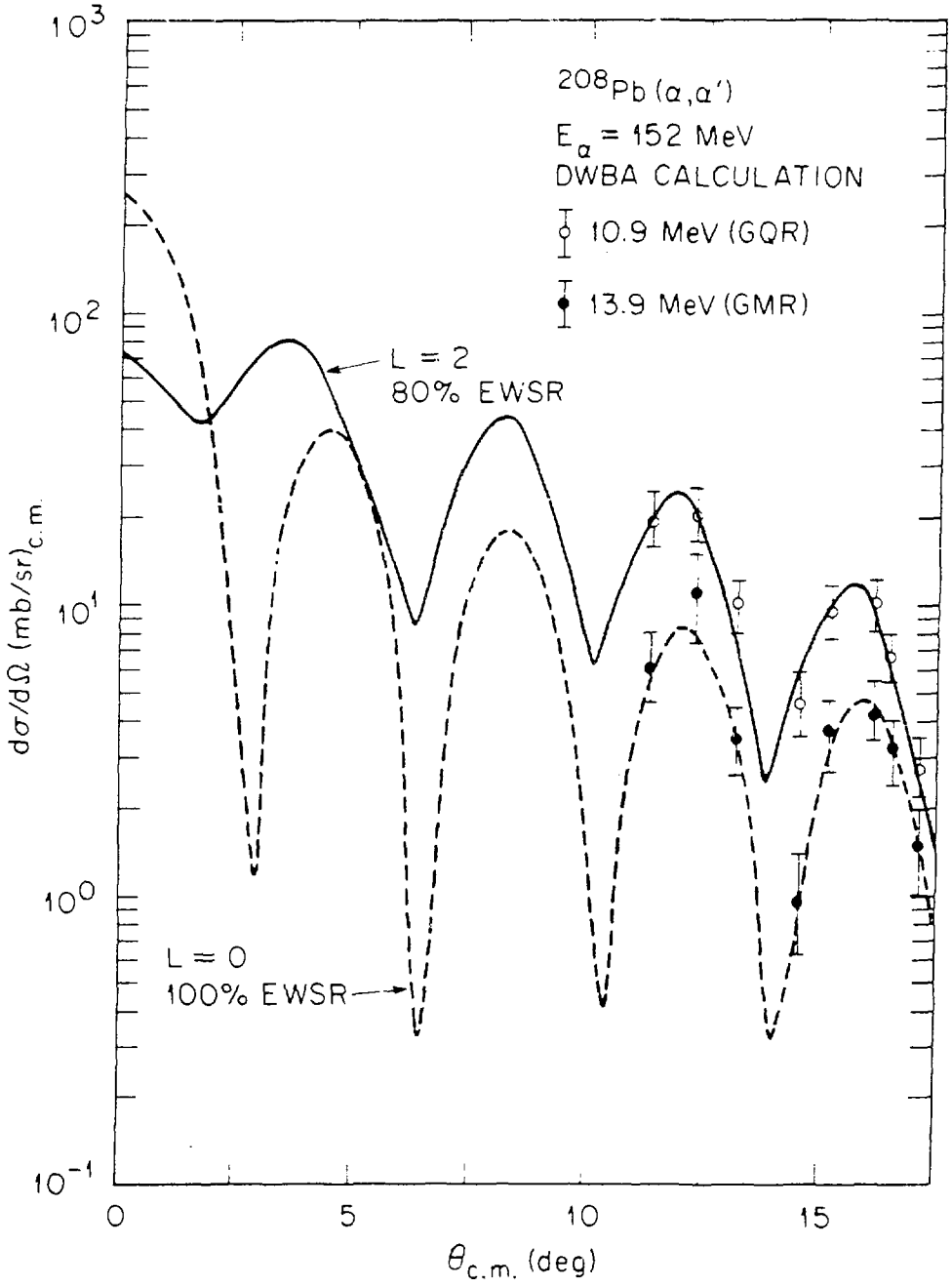

Fig. 14

ORNL-DWG 80-15700

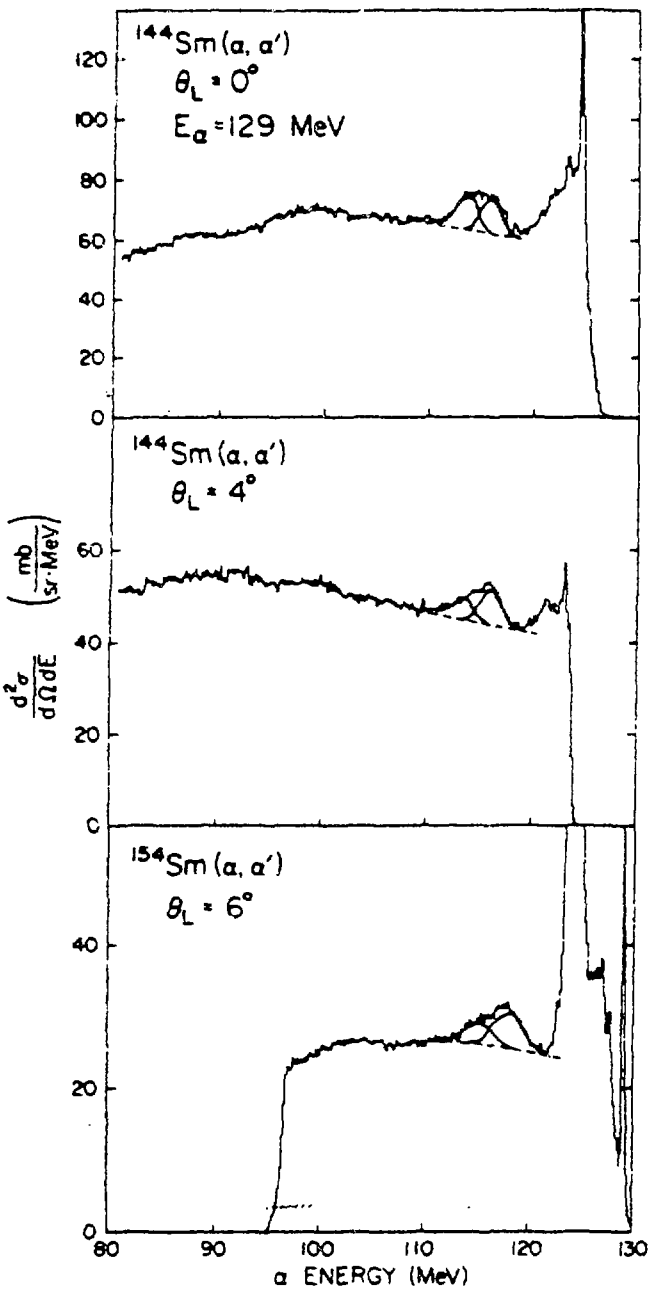

Fig. 15

ORNL-DWG 80-15699

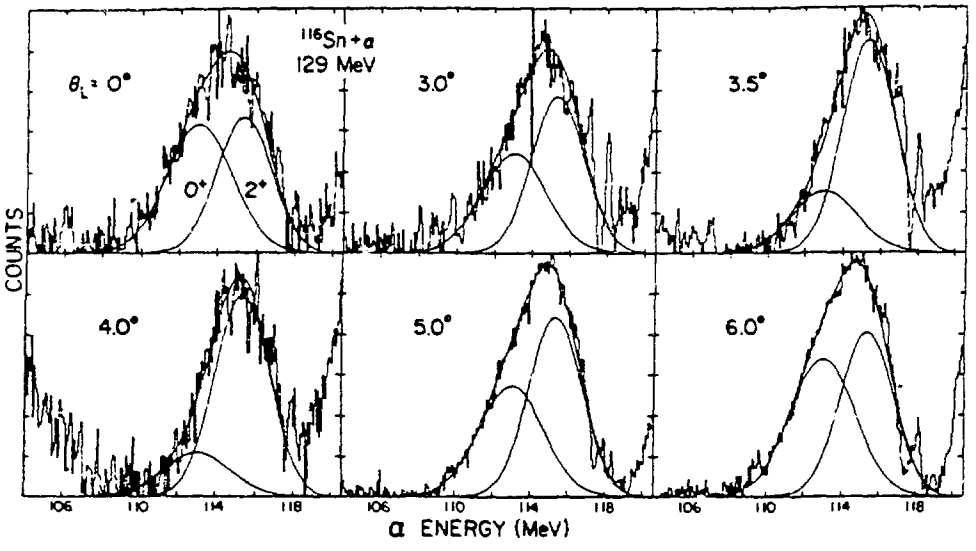

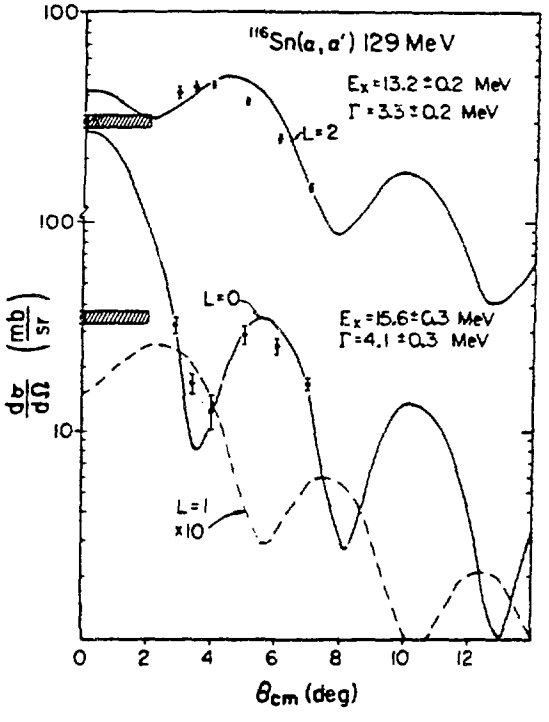

Fig. 16

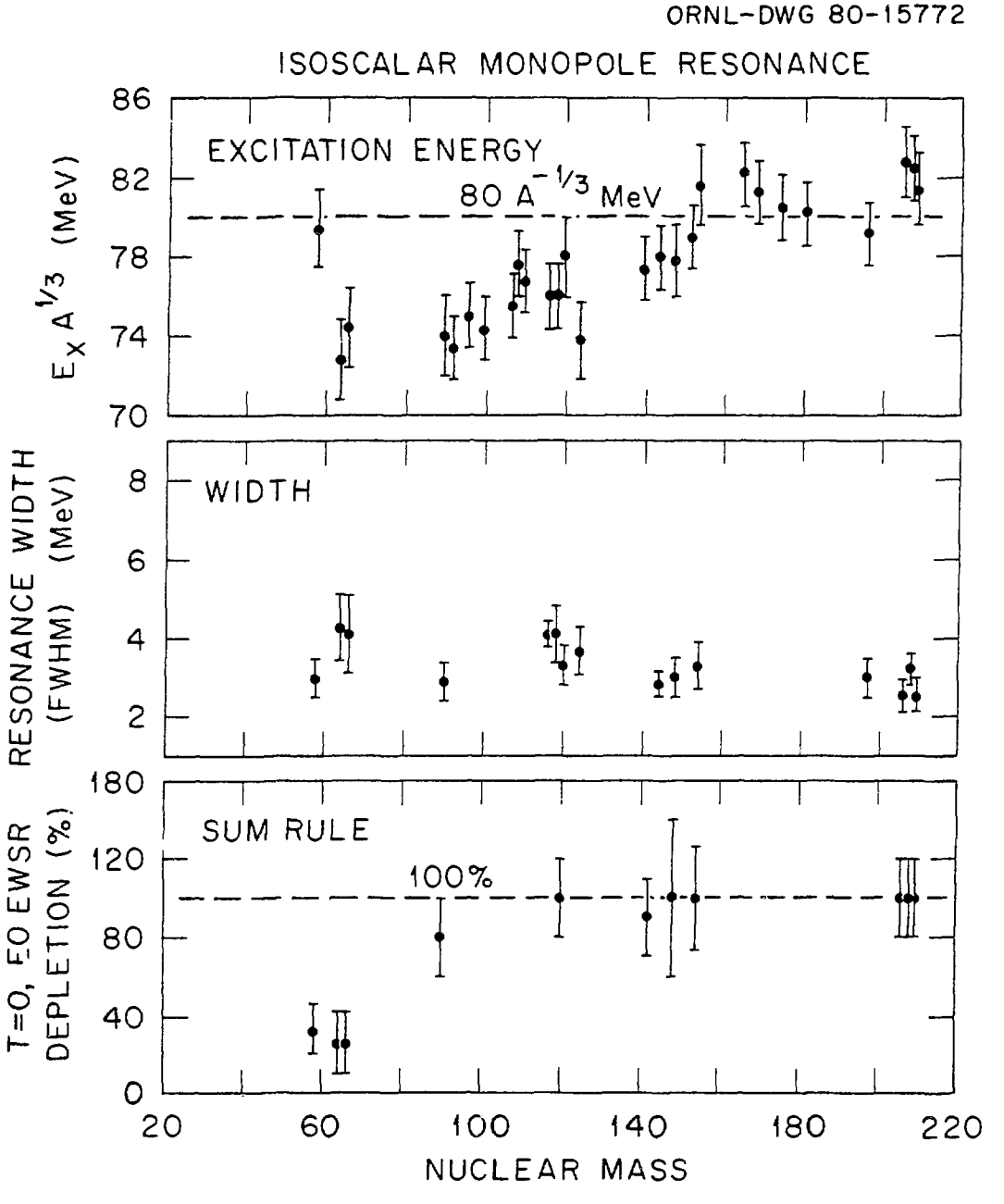
ORNL-DWG 80-15772
ISOSCALAR MONOPOLE RESONANCE
EXCITATION ENERGY
80 A^-1/3 MeV
E_X A^1/3 (MeV)
86
82
78
74
70
WIDTH
RESONANCE WIDTH (FWHM) (MeV)
8
6
4
2
SUM RULE
100%
T=0, E0 EWSR DEPLETION (%)
180
120
80
40
0
20
60
100
140
180
220
NUCLEAR MASS

Fig. 17

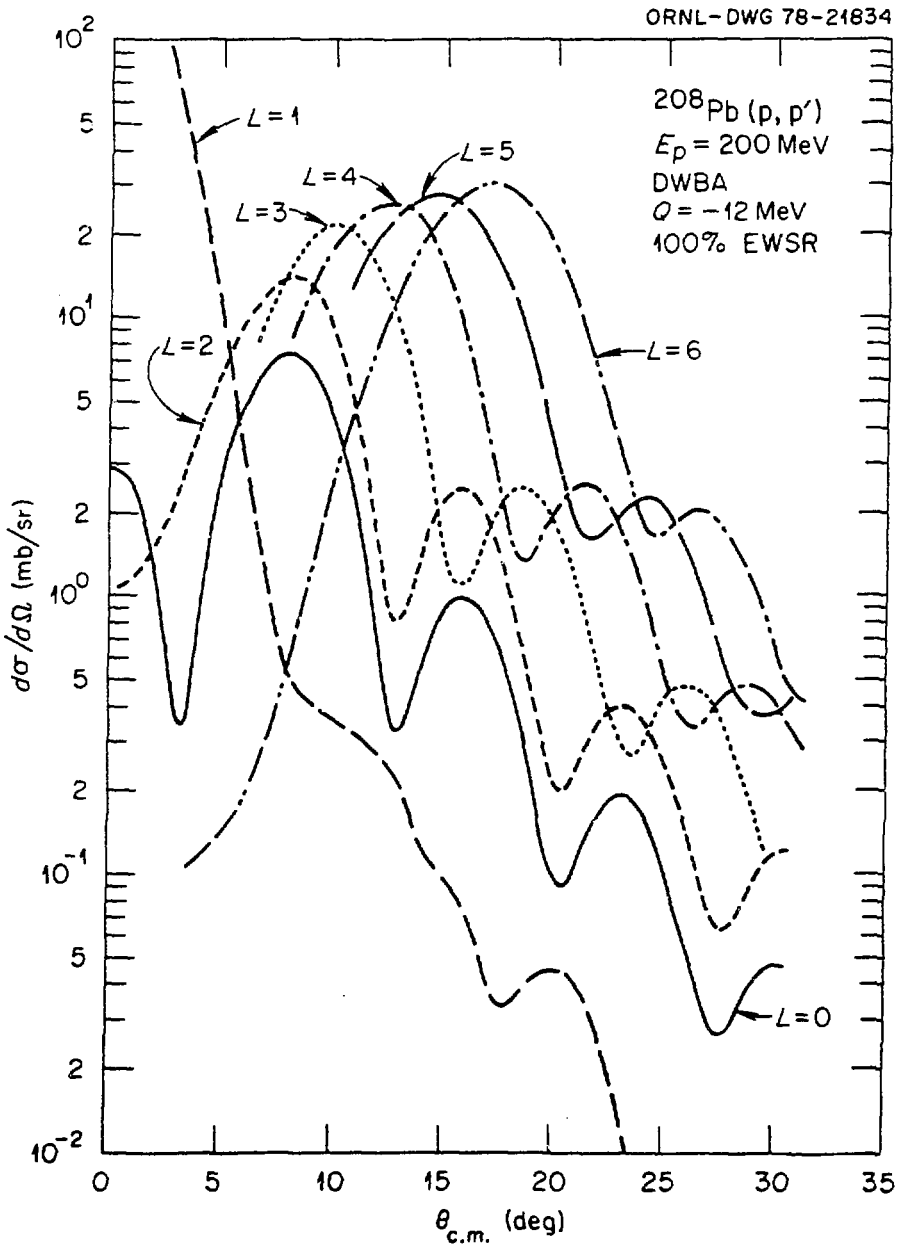
ORNL-DWG 78-21834
^{208}Pb (p, p′)
E_p = 200 MeV
DWBA
Q = −12 MeV
100% EWSR
L=1
L=2
L=3
L=4
L=5
L=6
L=0
$d\sigma/d\Omega$ (mb/sr)
$\theta_{c.m.}$ (deg)
10^2
5
2
10^1
5
2
10^0
5
2
10^{-1}
5
2
10^{-2}
0
5
10
15
20
25
30
35

Fig. 18

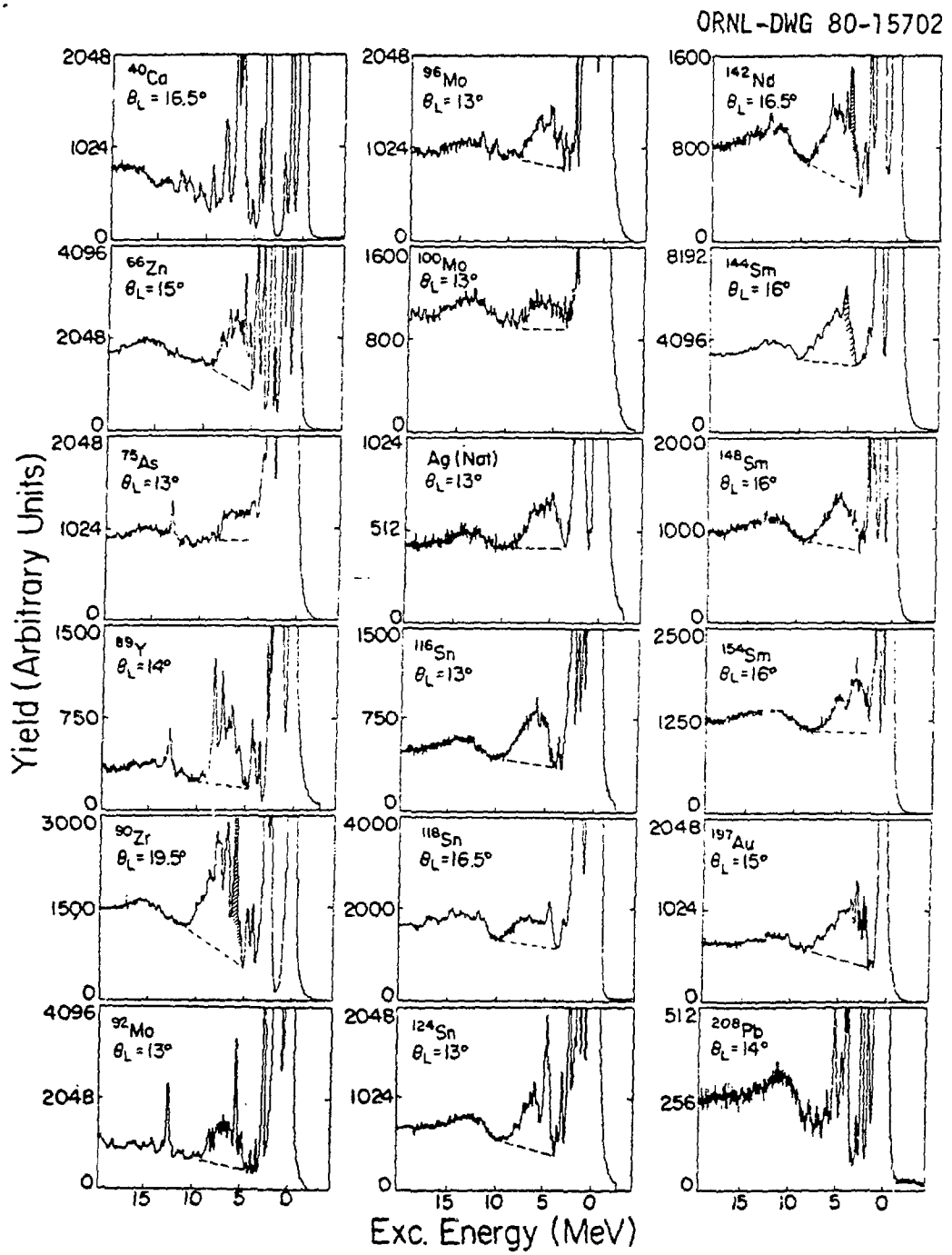
ORNL-DWG 80-15702
Yield (Arbitrary Units)
Exc. Energy (MeV)
40Ca θL = 16.5°
96Mo θL = 13°
142Nd θL = 16.5°
66Zn θL = 15°
100Mo θL = 13°
144Sm θL = 16°
75As θL = 13°
Ag (Nat) θL = 13°
148Sm θL = 16°
89Y θL = 14°
116Sn θL = 13°
154Sm θL = 16°
90Zr θL = 19.5°
118Sn θL = 16.5°
197Au θL = 15°
92Mo θL = 13°
124Sn θL = 13°
208Pb θL = 14°

Fig. 19

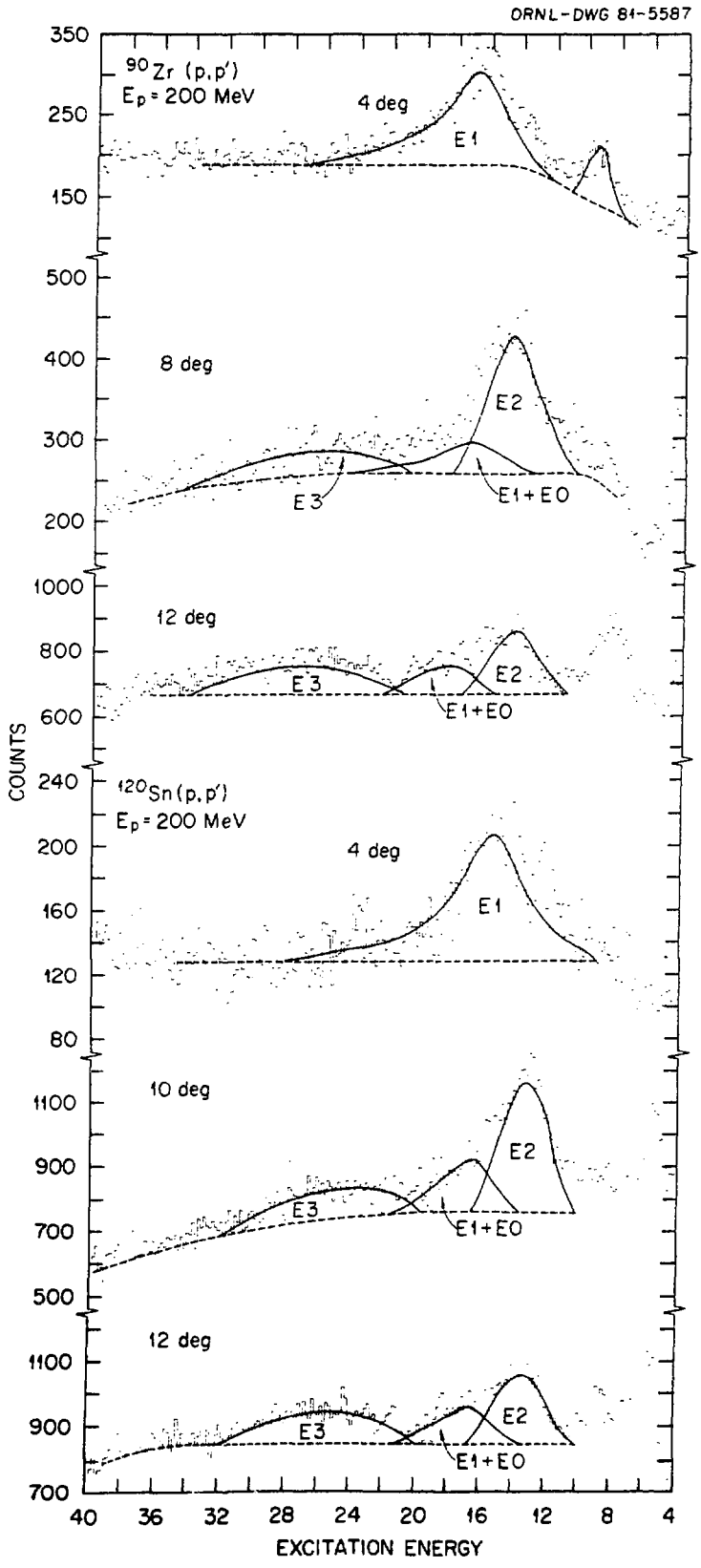
ORNL-DWG 81-5587
^{90}Zr (p,p')
E_p = 200 MeV
4 deg
E1
8 deg
E2
E3
E1+E0
12 deg
E3
E2
E1+E0
^{120}Sn(p,p')
E_p = 200 MeV
4 deg
E1
10 deg
E2
E3
E1+E0
12 deg
E3
E2
E1+E0
COUNTS
EXCITATION ENERGY

Fig. 20

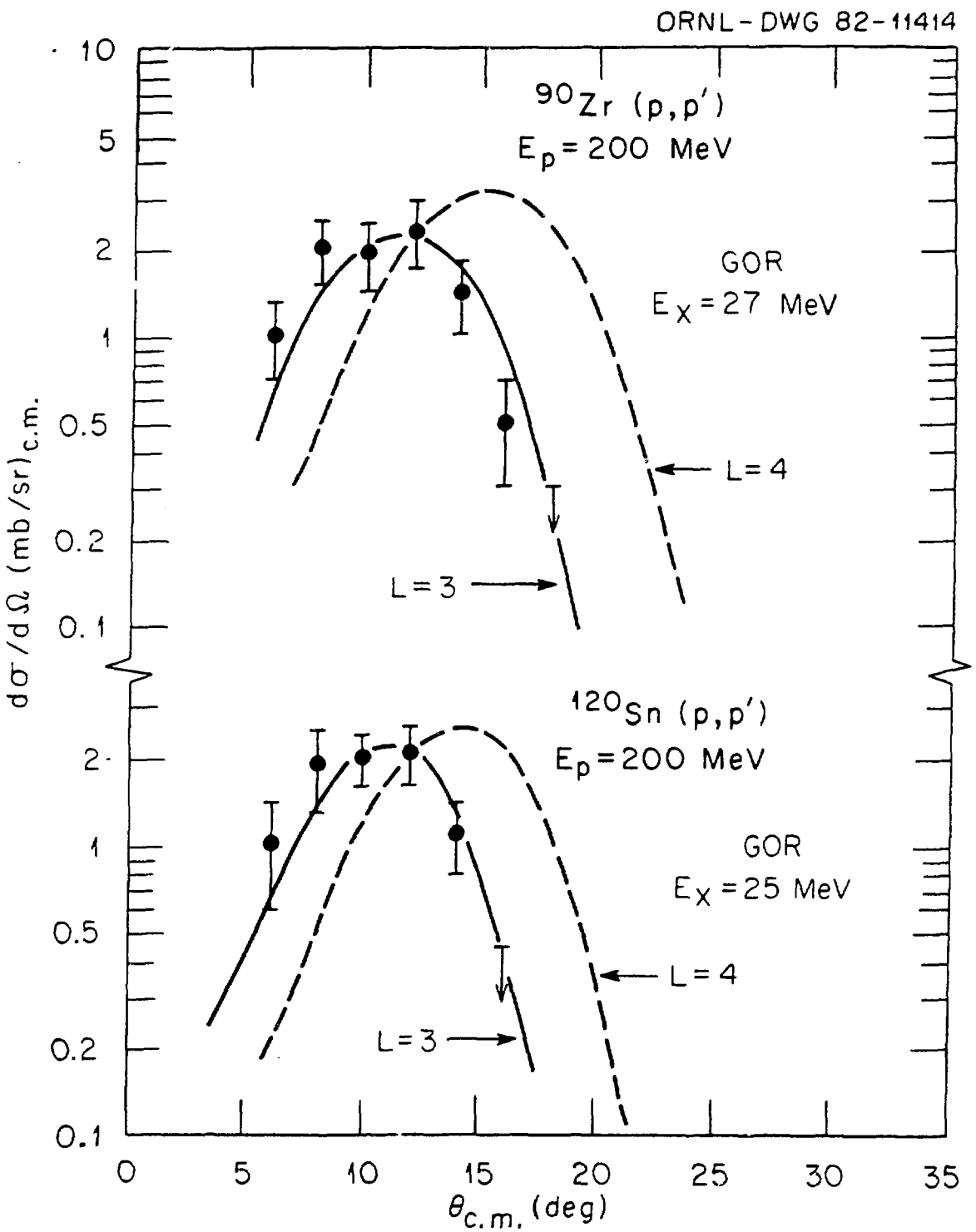
ORNL-DWG 82-11414
^{90}Zr (p,p')
E_p = 200 MeV
GOR
E_x = 27 MeV
L = 4
L = 3
^{120}Sn (p,p')
E_p = 200 MeV
GOR
E_x = 25 MeV
L = 4
L = 3
$d\sigma/d\Omega$ (mb/sr)$_{c.m.}$
$\theta_{c.m.}$ (deg)
10
5
2
1
0.5
0.2
0.1
0
5
10
15
20
25
30
35

Fig. 21

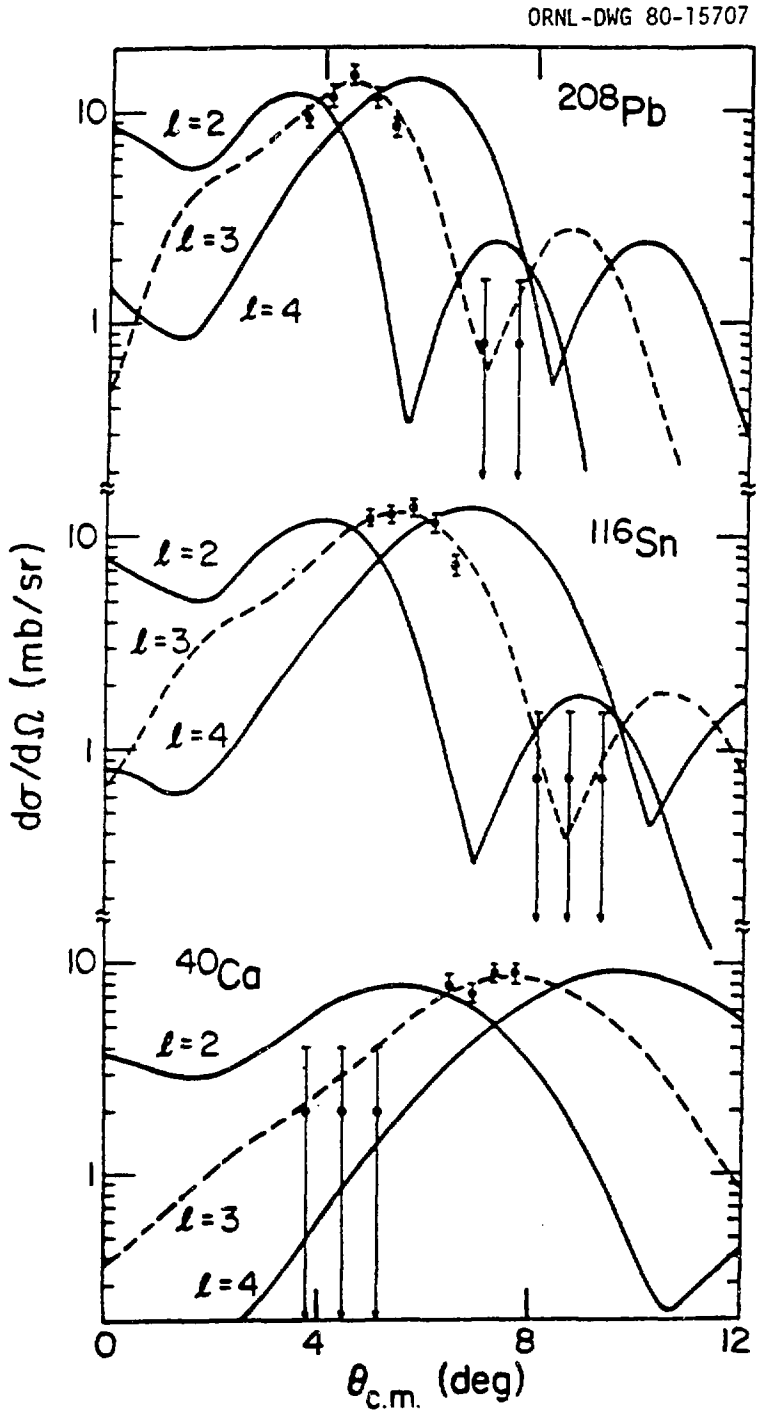
ORNL-DWG 80-15707
208Pb
116Sn
40Ca
ℓ=2
ℓ=3
ℓ=4
10
1
dσ/dΩ (mb/sr)
0
4
8
12
θc.m. (deg)

Fig. 22

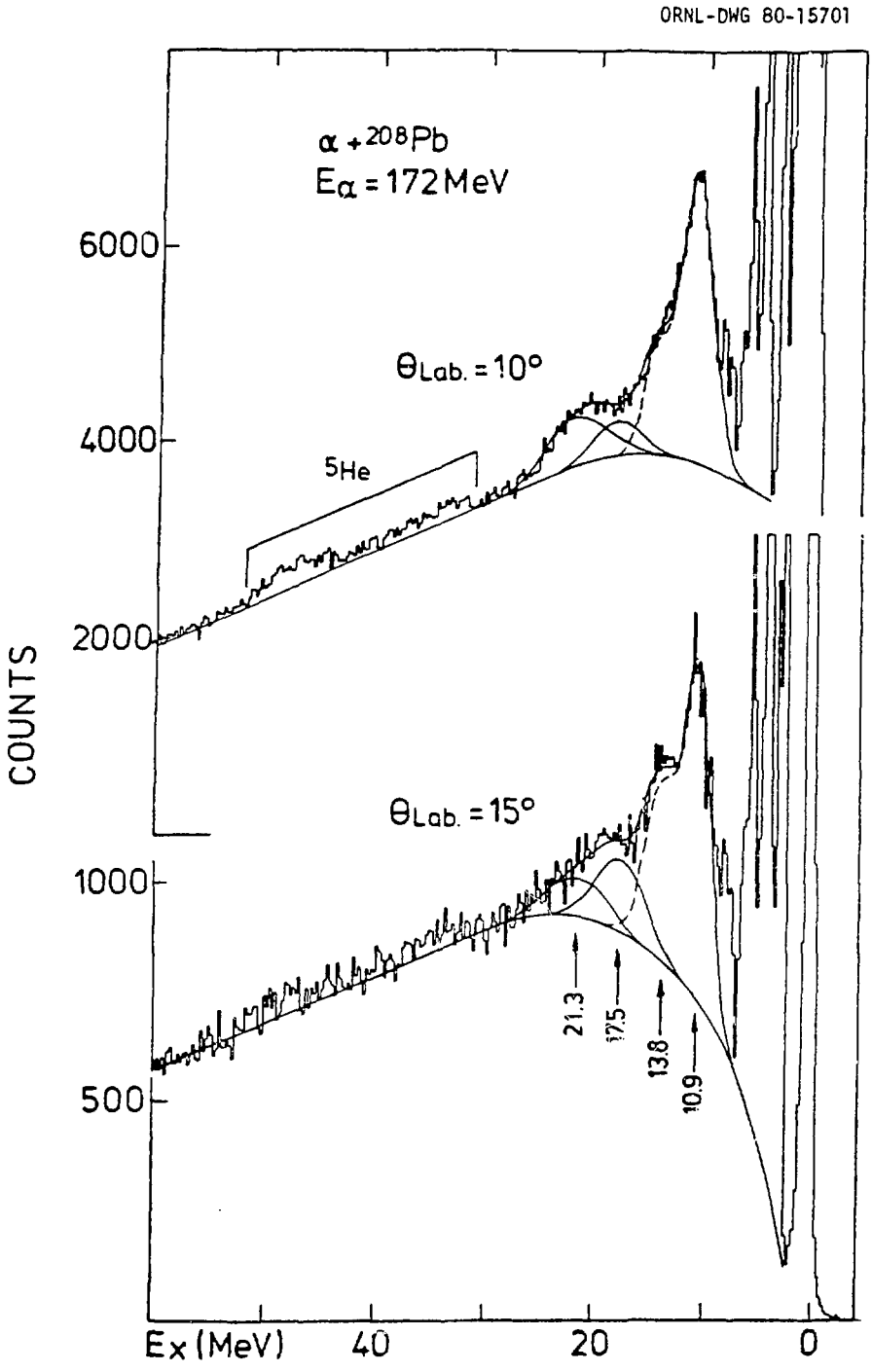
ORNL-DWG 80-15701
α + 208Pb
Eα = 172 MeV
θLab. = 10°
5He
θLab. = 15°
21.3
17.5
13.8
10.9
COUNTS
6000
4000
2000
1000
500
Ex (MeV)
40
20
0

Fig. 23

ORNL-DWG 80-15774R

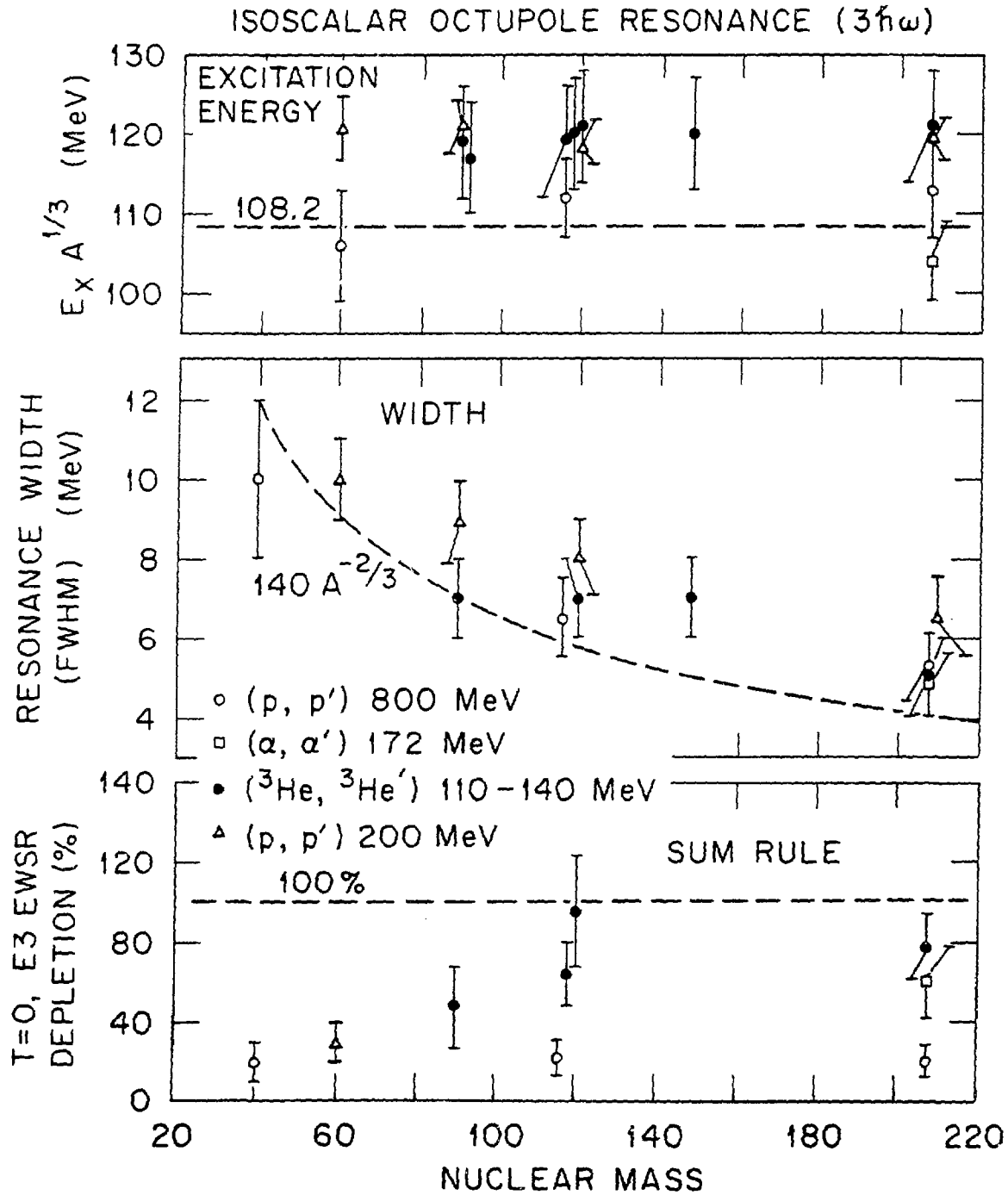

Fig. 24

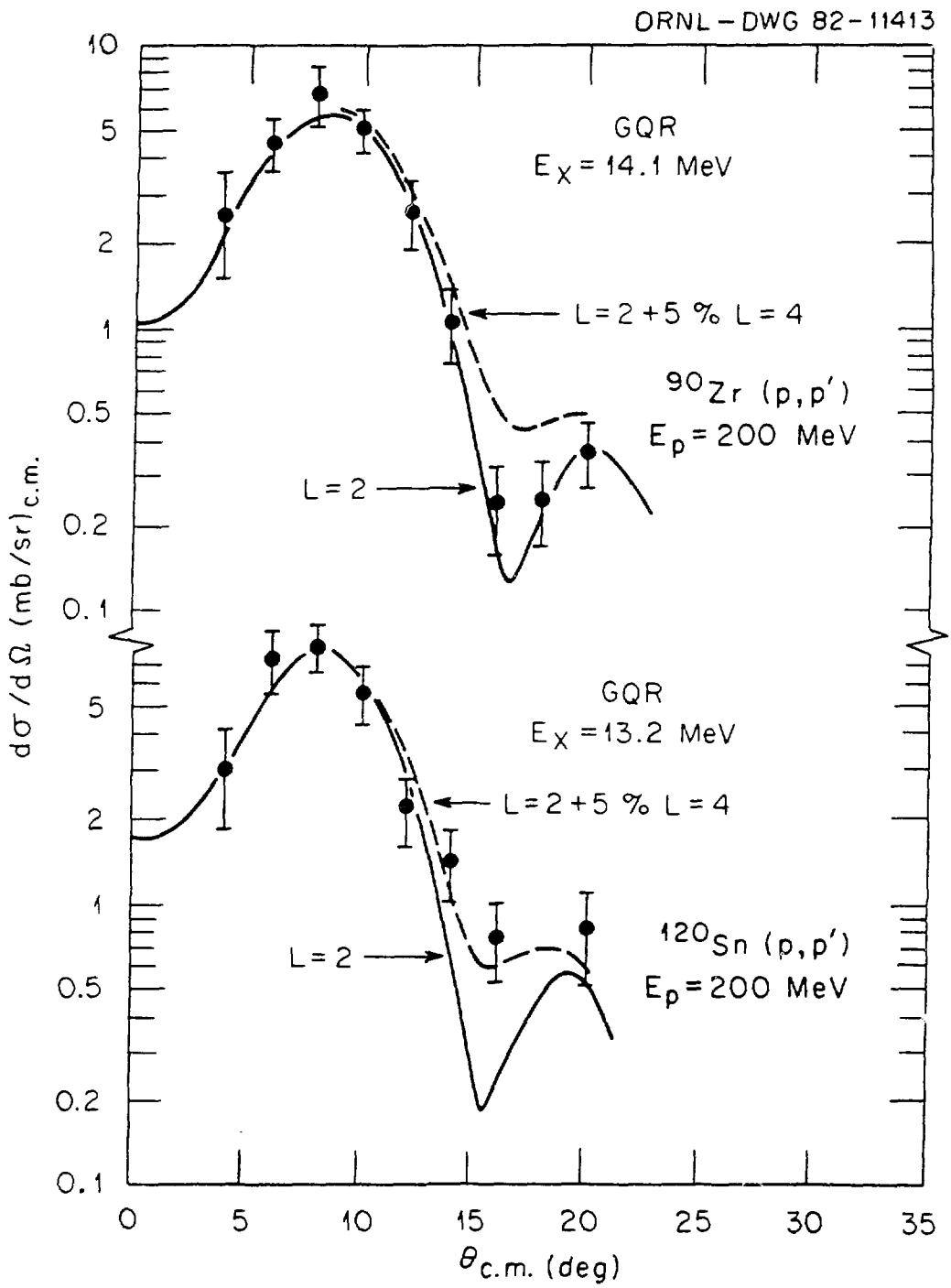
ORNL – DWG 82-11413
GQR
E_X = 14.1 MeV
L = 2 + 5 % L = 4
L = 2
^{90}Zr (p,p')
E_p = 200 MeV
GQR
E_X = 13.2 MeV
L = 2 + 5 % L = 4
L = 2
^{120}Sn (p,p')
E_p = 200 MeV
$d\sigma/d\Omega$ (mb/sr)$_{c.m.}$
$\theta_{c.m.}$ (deg)
10
5
2
1
0.5
0.2
0.1
0
5
10
15
20
25
30
35

Fig. 25

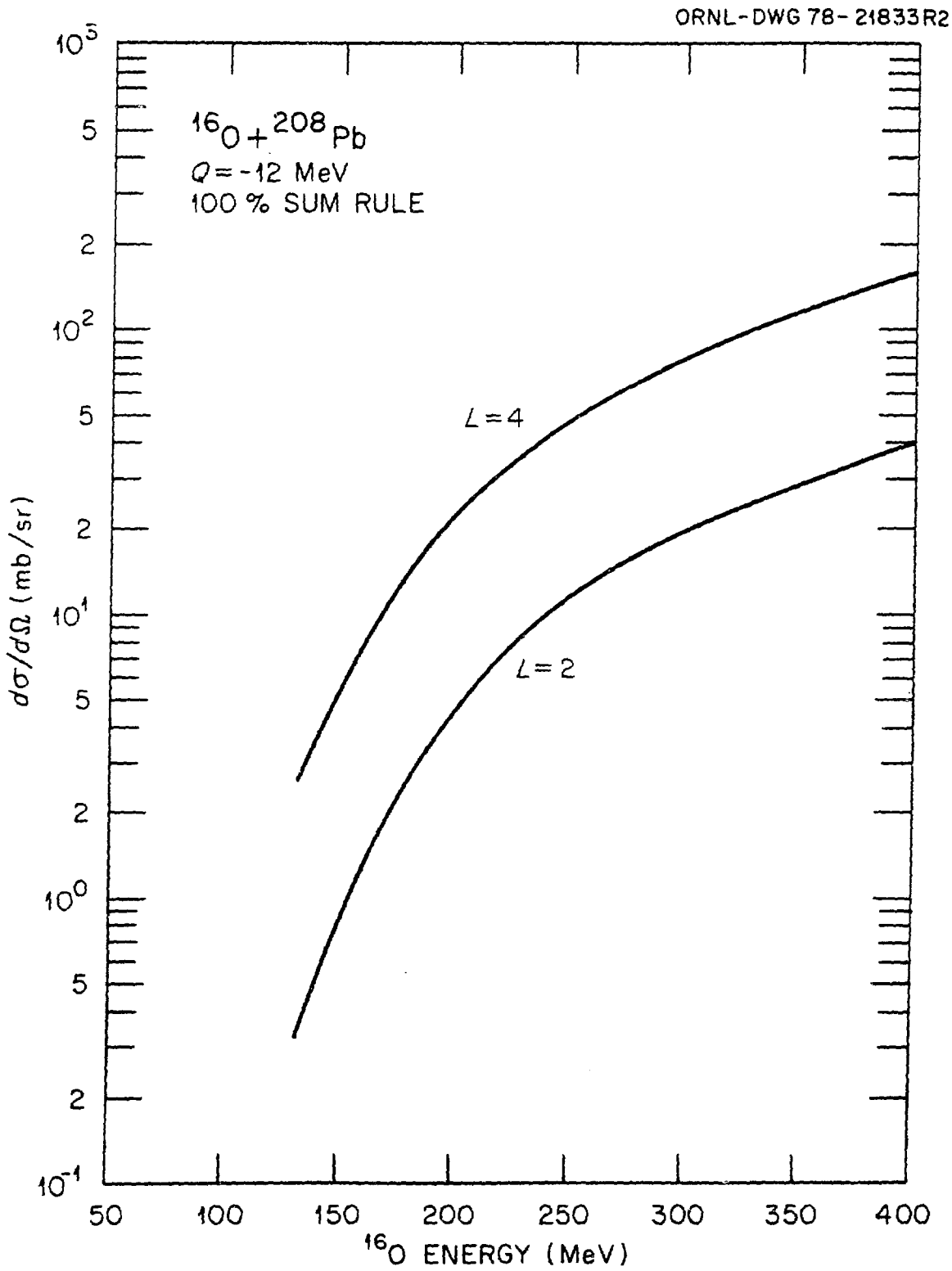
ORNL-DWG 78-21833R2
$^{16}O + ^{208}Pb$
Q = -12 MeV
100 % SUM RULE
L = 4
L = 2
dσ/dΩ (mb/sr)
^{16}O ENERGY (MeV)
10^5
5
2
10^2
5
2
10^1
5
2
10^0
5
2
10^{-1}
50
100
150
200
250
300
350
400

Fig. 26

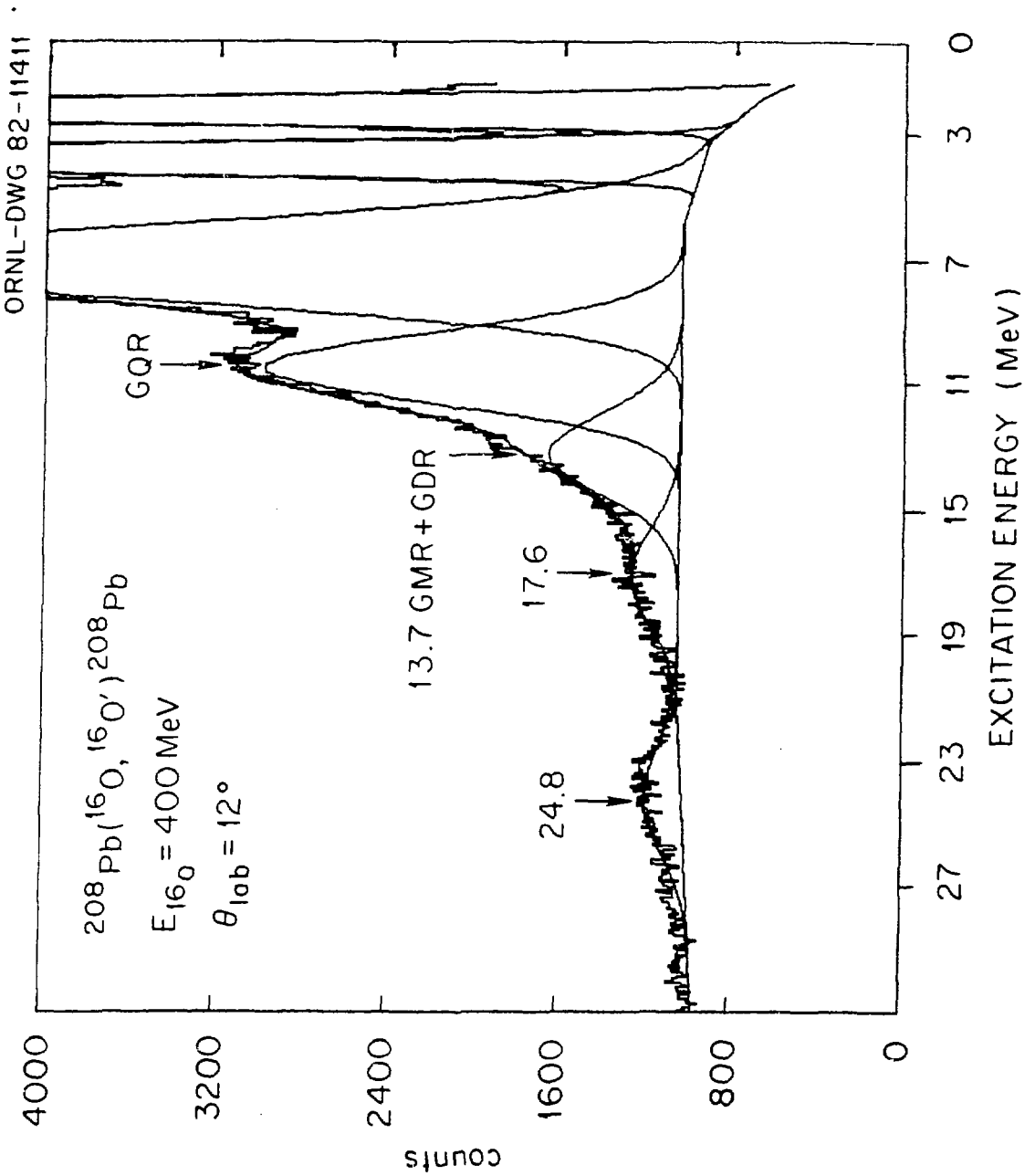
ORNL-DWG 82-11411
$^{208}Pb(^{16}O,^{16}O')^{208}Pb$
$E_{^{16}O} = 400$ MeV
$\theta_{lab} = 12°$
GQR
13.7 GMR + GDR
17.6
24.8
counts
4000
3200
2400
1600
800
0
27
23
19
15
11
7
3
0
EXCITATION ENERGY (MeV)

Fig. 27

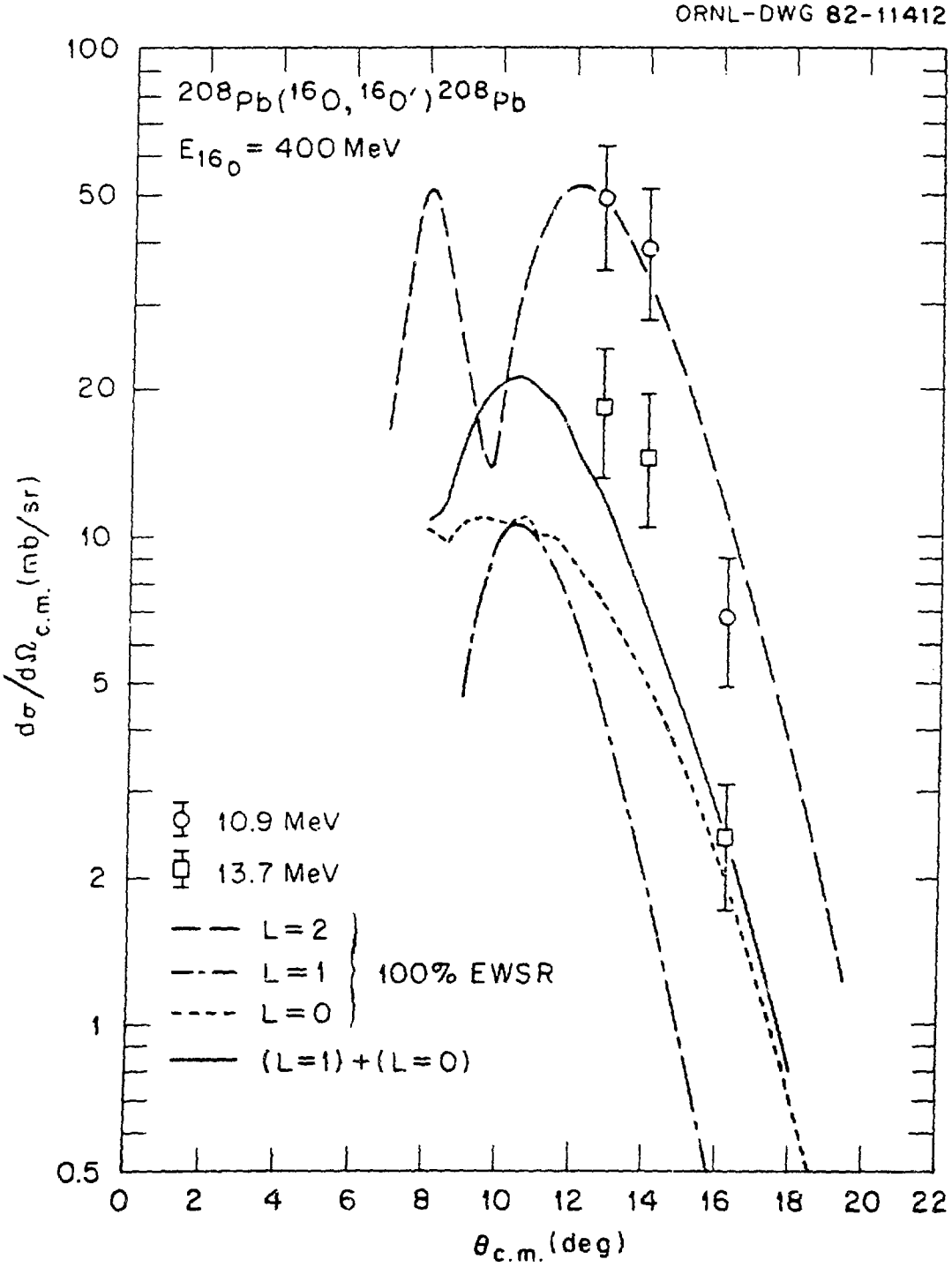
ORNL-DWG 82-11412
$^{208}Pb(^{16}O,^{16}O')^{208}Pb$
$E_{^{16}O}$ = 400 MeV
10.9 MeV
13.7 MeV
L=2
L=1
L=0
100% EWSR
(L=1)+(L=0)
$d\sigma/d\Omega_{c.m.}$ (mb/sr)
$\theta_{c.m.}$ (deg)
100
50
20
10
5
2
1
0.5
0
2
4
6
8
10
12
14
16
18
20
22

Fig. 28